CODIGEM

CORPORACIÓN DE DESARROLLO E INVESTIGACIÓN GEOLÓGICO-MINERO-METALÚRGICA

MINISTERIO DE ENERGÍA Y MINAS

DFID

DEPARTMENT FOR INTERNATIONAL DEVELOPMENT

BGS 1835

BRITISH GEOLOGICAL SURVEY

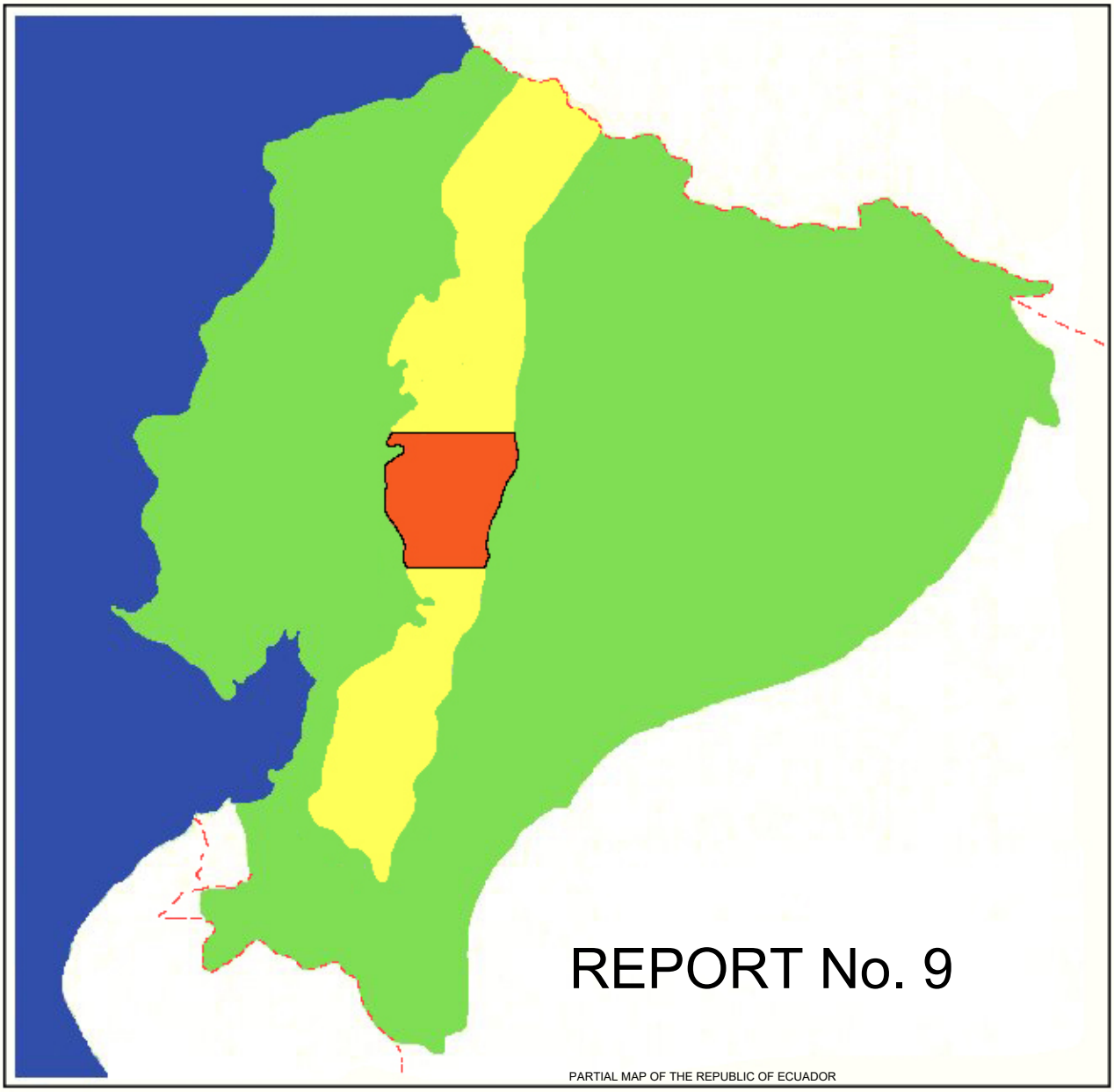

PARTIAL MAP OF THE REPUBLIC OF ECUADOR

REPORT No. 9

WORLD BANK MINING DEVELOPMENT AND ENVIRONMENTAL CONTROL PROJECT

GEOLOGICAL INFORMATION MAPPING PROGRAMME (WESTERN CORDILLERA)

PATRI MATRIQUE

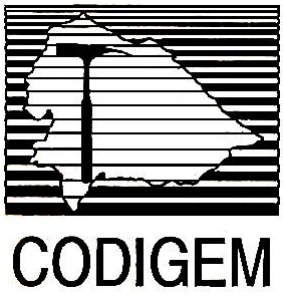

MINING DEVELOPMENT AND ENVIRONMENTAL CONTROL PROJECT

GEOLOGICAL INFORMATION MAPPING PROGRAMME

Report Number 9

GEOCHEMICAL RECONNAISSANCE SURVEY OF THE WESTERN CORDILLERA OF ECUADOR BETWEEN 1°00' AND 2°00'S

T. M. Williams

W. Castillo

E. Cruz

V. Acitimbay

CODIGEM-BRITISH GEOLOGICAL SURVEY

Quito-Ecuador

1999

Stalyn Paucar

2024 edition

GIMP GEOCHEMICAL SURVEY PROGRAMME
PARTICIPATING STAFF

Principal geochemist
Dr. T. M. Williams

Project leader
Dr. J. A. Aspden

CODIGEM
Mr. W. Castillo
Mr. E. Cruz
Mr. V. Acitimbay

FIELD OPERATIONS

N. Báez	J. Bolaños	E. López
M. Montero	G. Galarza	R. Rosales
H. Núñez	L. Pilatasig	F. Núñez
A. Tupipamba	J. Galarza	E. Hinojosa
F. Grijalva	L. Saltos	E. Romero
J. Segovia	R. Toro	M. Cruz

Reference

Williams, T., Castillo, W., Cruz, E. & Acitimbay, V. (1999). *Geochemical Reconnaissance of the Western Cordillera of Ecuador between 1°00' and 2°00'S* (Stalyn Paucar, Ed., 2024). Report Number 9. Geological Information Mapping Programme. BGS-CODIGEM/MEM.

CONTENTS

FIGURES

TABLES

1. INTRODUCTION

This report summarises the methodology and results of drainage geochemical reconnaissance of the 1°-2°S sector of the Western Cordillera of Ecuador, sampling of which was carried out during the period September 1996 to August 1998 under sub-component 3.4 (Thematic Mapping) of the *Mining Development and Environmental Control Project*. A digital data package for this area is available commercially, in accordance with the requirement of many prospective users to undertake independent data interpretation in a wide range of software applications.

2. AREA OF COVERAGE

The zone of survey coverage described in this report extends between longitudes 78°40'W-79°30'W and latitudes 1°0'-2°0'S (UTM SAD69 coordinates 680000-760000E and 9780000-9890000 N). The total area sampled is approximately 6750 km^2 (see cover illustration). Much of the eastern sector of the quadrangle is characterised by terrain in excess of 3000 m, including the highest location in Ecuador, the 6310 m Chimborazo stratovolcano. Drainage trends predominantly southward through the Río Salinas-Chimbo system, and westward via the Río Angamarca, Río Soloma-Sibimbi, Río La Plata systems (Fig. 1).

3. GEOLOGICAL SETTING

3.1 Overview

A 1:200000 scale geological map of the Western Cordillera sector 1°-2°S has been published by BGS-CODIGEM (1997). A detailed account of the lithostratigraphy, structure and mineralisation of the area is provided by McCourt et al. (1997), from which the following notes have been extracted. A simplified geological map, also based on this work, is provided in Fig. 2. Mapped sequences in the area range in age from Cretaceous to Quaternary. The oldest rocks are oceanic basalts of the Pallatanga Unit, found in tectonic contact with two sequences of turbidites: the Yunguilla Unit of Late Cretaceous age and the Apagua Formation of Eocene age. The latter is in tectonic contact to the west with the volcaniclastic Macuchi Unit of Paleocene to Early-Middle Eocene age. Along the eastern edge of the area, these rocks are unconformably overlain by intermediate to acid continental-margin calc-alkaline volcanic rocks of Mid- to Late Miocene age. The youngest rocks of the area are the products of Pliocene to Quaternary volcanism and Holocene sedimentation.

Faulting is ubiquitous, slicing the cordillera into a series of NNE-SSW-trending blocks. These are linked by a complex anastomosing fault system, bounded to the east and west by major deep-seated crustal structures: the Pallatanga Fault system and the Chimbo-Cañi Fault zone. Younger N-S trending faults, with a significant vertical component, also occur (e.g. the Río Chimbo Lineament). Folding, although most probably present in all the pre-Pliocene units, is most evident in the Yunguilla and Apagua sequences which are folded about N-S to NE-SW axes.

3.2 Pallatanga Unit (McCourt et al., 1997)

The Pallatanga Unit is a Cretaceous sequence of basic to ultrabasic rocks of oceanic affinity. Lithologies include basalt, basaltic volcanoclastics, microgabbro-diabase, peridotite and rare pillow lavas. The unit is exposed in the southeast of the area as a series of tectonic slices within the Yunguilla Unit and Apagua Formation.

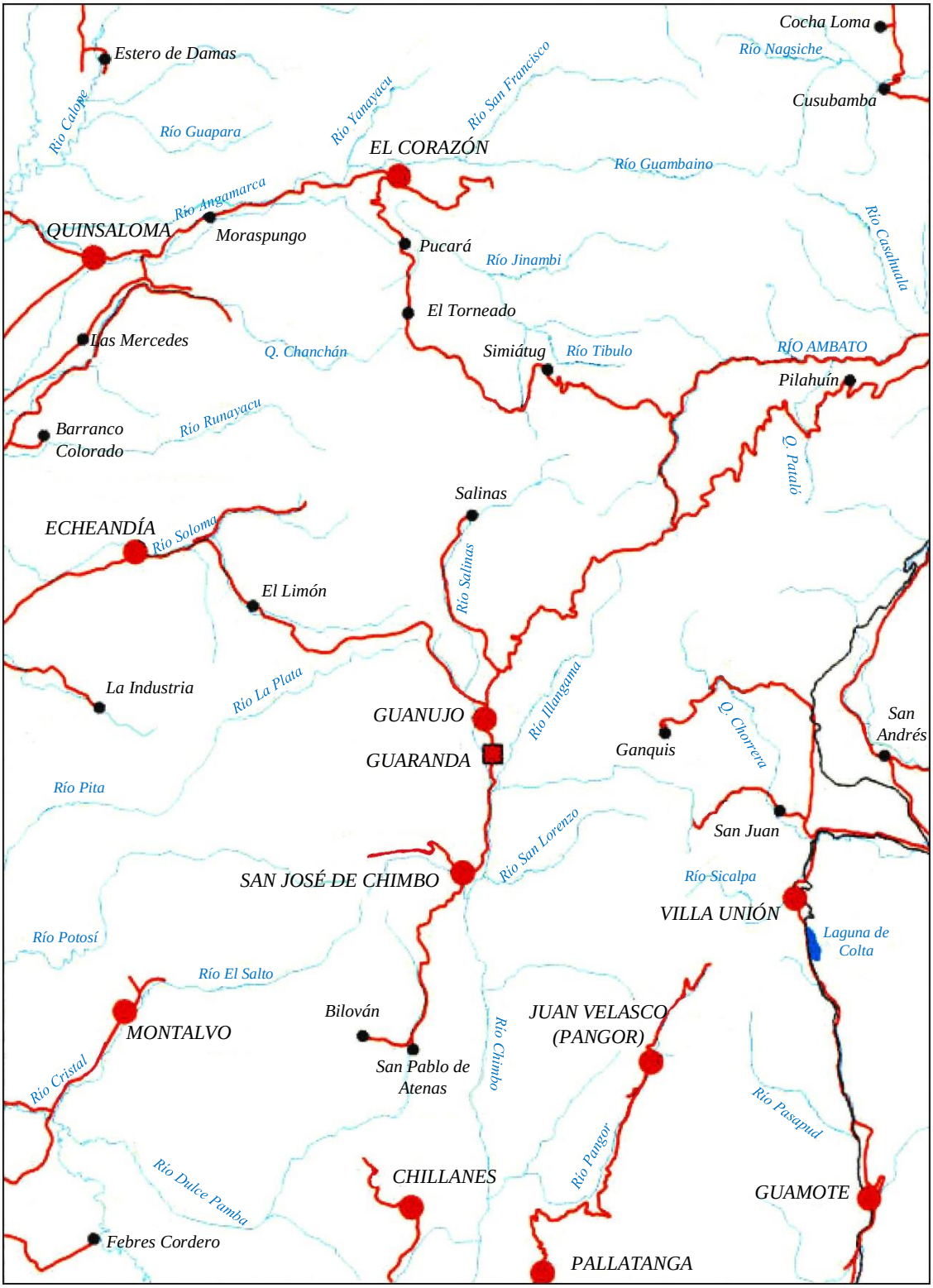

Figure 1. Western Cordillera 1°-2°S quadrangle: drainage, settlement and road network

3.3 Yunguilla Unit (cf. Yunguilla Formation, Thalmann, 1946)

The Yunguilla Unit is a sequence of fine-grained marine turbidites of Late Cretaceous age, characterised by thinly and irregularly bedded sediments. It crops out in the southeast of the area as a NNE-striking belt of width 0.65 to 11.0 km, occupying a structural position along the eastern margin of the cordillera adjacent to the Pallatanga-Pujilí Fault zone. The main lithologies are black-grey mudstones, locally calcareous siliceous black siltstones, fine-grained well-sorted sandstones, and grey limestones. The sequence is interpreted, at least in part, as having been deposited onto the Pallatanga Unit by turbidity currents soon after the accretion of the former against the continental margin.

3.4 Macuchi Unit (cf. Henderson 1979; Egüez, 1986)

The Macuchi Unit is an Early Tertiary volcanoclastic submarine arc sequence. It is exposed over some 35% of the 1°-2°S quadrangle and dominates the western half of the map. To the west it is in disconformable contact with quaternary deposits. To the east its main contact is with the turbidites of the Apagua Formation. This latter contact is interpreted as a major fault, juxtaposing two broadly contemporaneous but lithologically distinct sequences. The main rock types recognised are (in order of abundance) volcanic sandstones, breccias, tuffs, volcanic siltstones, cherts, pillow breccias, hyaloclastites, diabase-microgabbro, sub-porphyritic basalts and calcarenites. Geochemical analyses of six samples (McCourt et al., 1997) indicate a predominantly subalkaline basalt or basaltic andesite composition with tholeiitic calc-alkaline characteristics. All the samples have normative quartz and low Ti/V ratios, typical of island arc basalts.

3.5 Angamarca Group (Hughes and Bermúdez, 1997)

The Angamarca Group comprises the Pilaló, Apagua, Unacota, Rumi Cruz and Gallo Rumi Formations. The total thickness of the sequence is ca. 4000 m, deposited from the Paleocene to the Late Eocene. The clastic turbidites of the Apagua Formation are the dominant lithology, and throughout most of the area define the main faulted contact with the volcanoclastic Macuchi Unit to the west. The Angamarca Group is interpreted as being deposited in a marine delta-fan environment, with mature clast material derived from reworking of a fluvial hinterland source. This model implies uplift and may indicate a major tectonic event in the Late Eocene. Although the source area for the sediments is unproven, the high percentage of quartz supports a continental sialic hinterland.

3.6 Arrayanes Unit (McCourt et al., 1997)

The Arrayanes Unit is a sub-horizontal, sequence of fine-grained sediments and basaltic andesite to andesitic lavas of probable latest Eocene age. It is present only within the area of the Macuchi outcrop. It comprises regular bedded siliceous mudstones and fine-grained quartz-arenites, mafic-rich green fine-grained volcanic sandstones with subordinate tuffs, and intercalated aphyric basalts or plagioclase-phyric sub-porphyritic basaltic-andesites. Contacts with the underlying Macuchi Unit are poorly exposed but appear to be discordant. The Arrayanes Unit is tentatively interpreted as a sequence of distal turbidites, deposited onto the Macuchi allochthonous block either following or during its accretion to the South American Plate. The sediments may be derived, in part, from erosion of the emergent arc, and the volcanics represent the final stages of activity of the arc.

3.7 Saraguro Group (undifferentiated; Dunkley and Gaibor, 1997)

The Saraguro Group is a sequence of intermediate to acid, calc-alkaline, sub-aerial volcanic rocks with important (ignimbritic) welded tuff horizons at the top and andesitic lavas towards the base. It correlates, in part, with the Saraguro Formation of Kennerley (1973), and the Saraguro Group of Baldock (1982). Much of the group is assigned an Oligocene age, with an overall range from the Late Eocene to Early Miocene (38.6-22.8 Ma). In the 1°-2°S area, the outcrop is confined to a north-south strip some 20 km long and 2-4 km wide, exposed along the Macuchi-Apagua contact to the east of Guaranda. Lithologies comprise a mixture of grey-green porphyritic, plagioclase ± hornblende-phyric, andesitic lavas, breccias and tuffs, the latter with shards. They disconformably overlie the Apagua Formation and are unconformably overlain by younger volcanic rocks of the Zumbagua Group. The Saraguro Group is considered to be the result of continental margin volcanism which followed the accretion of the Macuchi arc terrane.

3.8 Zumbagua Group (Hughes and Bermúdez, 1997)

The Zumbagua Group comprises volcanic and volcano-sedimentary rocks of Middle to Late Miocene age. The sequence covers much of the northeast part of the map, unconformably overlying the Apagua, Arrayanes and Macuchi units, as well as the Saraguro Group. It is locally overlain unconformably by Plio-Quaternary volcanics. The lithologies are predominantly coarse-grained, comprising very poorly sorted sandstones and unsorted debrite breccias in beds up to several metres thick. In addition, plagioclase-phyric, greyish andesitic to dacitic tuffs are present in the western part of the sequence, overlain by spectacular horizontal composite laharic units over 40 m thick around Salinas.

3.9 Cisarán Formation (Dunkley and Gaibor, 1997)

Within the 1°-2°S quadrangle, the Cisarán Formation (Late Miocene) extends south from Chimborazo to the limit of the area. It is best exposed along the track from Pallatanga to El Olivo [7341-97802], where plagioclase-phyric andesitic lavas and tuffs, formerly included in the Alausí Formation, are overlain by tuffaceous sandstones and fine-grained green to purple volcanic sandstones and siltstones. The Formation overlies and blankets the pre-existing topography of the Saraguro Group, and is overlain by Quaternary ash and pumice deposits.

3.10 Undifferentiated Plio-Pleistocene volcanics

Undifferentiated Plio-Pleistocene volcanics include the post-Zumbagua sequence formerly referred to as the *Volcánicos Lourdes* and *Volcánicos de Sagoatoa* (DGGM, 1978-1979). The former crop out to the west and southwest of San Miguel de Bolívar, comprising deeply weathered acid lithologies with large quartz ± feldspar phenocrysts. They show extensive hydrothermal argillic alteration, silicification and sulphide (chalcopyrite-pyrite, ± bornite) mineralisation. Similar lithologies are present southwest of Sicoto, but with no analogous hydrothermal alteration. The Volcánicos de Sagoatoa are exposed to the northwest of Ambato and comprise lavas and subordinate tuffs.

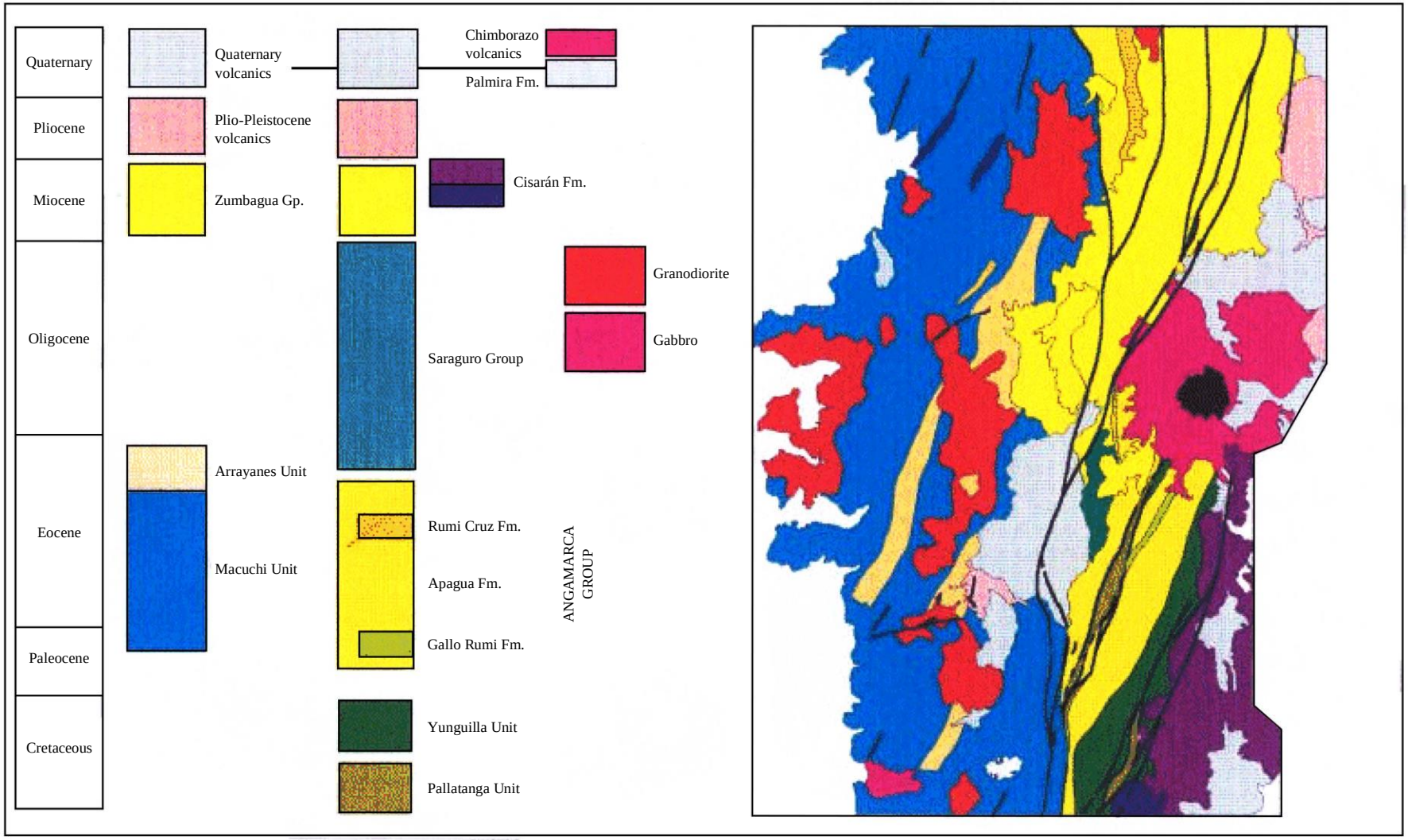

Figure 2. Simplified geology of the 1°-2°S sector of the Western Cordillera of Ecuador. The stratigraphy on the left of the legend depicts the area west of the Chimbo-Cañi Fault System. The stratigraphy on the right depicts the area to the east. The position of intrusive rocks within the legend has no stratigraphic significance

3.11 Undifferentiated Quaternary Volcanics

Undifferentiated Quaternary Volcanics correspond primarily to the *Volcánicos Cotopaxi* of BGS-CODIGEM (1993a) and the combined Cangagua Formation, Altar and Cotopaxi Groups of Baldock (1982). The sequence includes Pleistocene air-fall tuffs, breccias and agglomerates, and andesitic lavas from the older centres of Chimborazo, Carihuairazo and the Illinizas. These are covered by volcanic ash, pumice, debris flows and minor lavas derived from younger volcanoes and volcanic centres such as Cotopaxi, Tungurahua, Pululahua and Quilotoa. The products of the older centres are mainly andesitic, whereas the younger ones are more variable with early phases of dacitic activity followed by a major andesitic phase finally basaltic flows.

3.12 Chimborazo and Carihuairazo Volcanics

Eruptive products of Chimborazo include lavas, pyroclastic flows, debris avalanches, lahars and ash-fall deposits. They vary in composition from basaltic andesites to hornblende-bearing dacites, with an SiO_2 range of 56-65% (Hall and Mothes, 1994). Eruptive activity at Chimborazo and Carihuairazo was most probably initiated in the Early Pleistocene. The Carihuairazo and oldest Chimborazo lavas comprise porphyritic pyroxene-andesites. The younger Chimborazo lavas are confined to the southeastern flanks and comprise vesicular pyroxene-phyric andesites and rare dacites. The youngest products of Chimborazo are located along its western flanks, comprising scoriaceous and pumiceous, coarse-grained tuffs containing feldspar, pyroxene, magnetite and andesitic lithics, andesitic-dacitic lavas and debris flows/lahars.

3.13 Quaternary alluvial and colluvial deposits

Holocene alluvium blankets the major river valleys. Occasional older river terraces are present locally, for example along the Río Chimbo. Extensive colluvium deposits, including alluvial cones, occur along the western margin of the cordillera.

3.14 Intrusive rocks

Plutons and minor intrusions are present throughout the mapped area, but are most prominent within the western half. The four largest are, from north to south, the El Corazón, Echeandía (La Industria), Chazo Juan and Balzapamba plutons. In general terms all intrusions can be divided into two groups: major plutons of calc-alkaline I-type granitoids emplaced within the Macuchi volcanoclastic sequence, and porphyritic and microtonalitic dykes, sheets and stocks intruding the flysch and younger volcanic sequence, often along fault structures.

Whole-rock geochemical data for the granitoids of the 1°-2°S area show a compositional range from quartz diorite-tonalite to granodiorite. On the tectonic classification plots of Whalen et al. (1987) and Pearce et al. (1984) they plot as orogenic volcanic arc granitoids. On normalized spidergrams they show LIL enrichment, with depletion of Nb, Ti and Y-Yb. The latter is typical of calc-alkaline magmas formed in a subduction setting. K/Ar dating of 32 hornblende and/or diorite samples suggests emplacement of the major intrusions from the Early Oligocene to the Middle Miocene (34-14 Ma) with major pulses at 34-30 Ma, 26-19 Ma and 16-14 Ma.

A major gabbroid body is present in the extreme southwest of the area. It comprises a mixture of lithologies including gabbro, quartz-gabbro, hornblende diorite, microgabbro and hornblende-pegmatites. Gabbroic rocks, particularly microgabbro-diabase, are also relatively common throughout the Macuchi Unit outcrop.

3.15 Structure

The Western Cordillera is limited to the east and west by deep-seated faults, interpreted as sutures. To the west it is approximately defined by the north-northeast-trending Guayaquil-Babahoyo-Santo Domingo-Fault zone (Baldock, 1982) which extends into Colombia as the El Tambor-Río Mira Fault. To the east, it is bounded by the complex north-northeast trending Calacalí-Pallatanga Fault zone (Aspden et al., 1987), and its extension into Colombia the Cali-Cauca-Patía Fault (McCourt et al., 1984). Within the Cordillera, elongate fault-bounded blocks define several distinct terranes.

Within the 1°-2°S area, the main north-east trending structures occur in the southeast of the mapped area, forming part of the Pallatanga Fault System. North of Pallatanga, the principal component of this system is renamed the Pangor Fault, a sub-vertical, easterly dipping local reverse fault along which rocks of the ophiolitic Pallatanga Unit have been thrust westwards over the Yunguilla Unit.

To the west of the main fault zone there are numerous parallel fault sets, the most important of which the Tambillo Fault extends from the southern margin of the quadrangle to the Chimborazo stratovolcano. This structure is interpreted to a satellite fault of the Pallatanga system, possibly reactivated during Miocene to Pliocene time and coinciding with the development of the principal intermontane basins of southern Ecuador. Immediately to the west of the Tambillo Fault, the Río Chimbo Lineament is interpreted to form part of an extensive Late Eocene suture related to the accretion of the Macuchi terrane to continental South America.

3.16 Metalliferous mineralisation

There is relatively little-known economic mineralisation in the area. The main areas of interest with respect to base and precious metal mineralisation were identified during the San Miguel Project undertaken by DGGM (now CODIGEM) and IGS (now BGS) from 1975-1979. Several prospects for porphyry copper ± gold-molybdenum mineralisation were identified and recommended for further investigation (Aucott et al., 1979). Almost all are related to granitoid intrusions or their contacts with the Macuchi Unit. Limited follow-up led to the identification of nine priority interest areas within the 1°-2°S sector: Chazo Juan [706-9846], La Industria-Yatubi [688-9826], Tres Hermanas [700-9826], Telimbela [704-9816], Balzapamba [703-9805 to 708-9808], San Miguel [716-9808], Las Guardias [708-9800], Sicoto [712-9798] and Tambillo [723-9784]. All of these areas were evaluated and the most promising were followed up, as part of the Bolívar Project (Phases I-III) carried out by JICA and INEMIN (now CODIGEM) between 1988-1991. This included drilling at El Torneado [708-9808], Osohuayco [7075-9806] and NE Telimbela at Ashuaca [7056-98172].

4. SAMPLING AND ANALYTICAL PROCEDURES

4.1 Numbering system

A random numbering system based on that of Plant (1973) and Garrett (1983) was deployed throughout the Western Cordillera geochemical survey to preclude analytically-induced campaign boundaries (within or between sheet areas) and/or the generation of spurious multiple-sample anomalies. Prior to sampling of the project area, several thousand sample bags were sequentially numbered, randomized and issued. On return to the CODIGEM laboratory, all filled sample bags were re-ordered and forwarded for analysis in sequential batches of ca. 120 samples. Through this procedure short-term analytical fluctuations (affecting one or more sample batches) are manifested as analytical noise across the entire project area, rather than as discrete local or sub-regional trends.

4.2 Field sampling procedure

Drainage sediment samples were collected by two sampling teams, each comprising eight trained prospectors. Samples were collected during five commissions, each lasting three weeks, during dry season conditions (May-December). A total of 2150 samples were collected from a ca. 6700 km^2 area, representing an average resolution of 1 sample per 3.1 km^2. In all instances emphasis was placed on the recovery of samples from first or second order regimes, thus constraining relatively small provenance areas.

The sampling methodology deployed throughout the Western Cordillera survey was derived from that of Plant and Moore (1979), and is broadly compliant with the global IGCP 259/360 protocol for International Geochemical Mapping (Darnley et al., 1995). Sampling stations were located upstream of potential sources of perturbation (habitation, industrial activity, agricultural discharges or bridging structures). At each site several kilograms of active channel detritus were collected following the removal of the hydrous-oxide enriched interfacial horizon. The alluvium was then wet-screened through an 80 BSI mesh (177 μm) sieve using a minimum volume of water so as to avoid the loss of fine silt and clay fractions. Following a settling period of ca. 20 minutes, the clear water overlying the sediment was decanted and approximately 100 g of the remaining sediment transferred to a pre-numbered kraft bag for transport and storage.

The selection of an 80 BSI sediment fraction for use throughout the survey was based on an orientation study by Dunkley et al. (1997) in the Río Junín basin. The fraction effectively reflects both mechanical and hydromorphic dispersion signatures (e.g. Williams et al., 1992) and avoids the logistic problem of collecting a sufficient mass of finer (100 BSI or smaller) material from the high-energy drainage systems which characterise much of the higher ground of the Western Cordillera.

4.3 Sample preparation

On return from the field all samples were air-dried at <40°C thus precluding any loss of Hg or other volatile elements. Samples were then disaggregated with a pre-washed pestle and mortar to yield a fine homogeneous powder. This was sub-sampled using a cone-and-quarter technique to produce a ca. 50 g aliquot for multi-element analysis.

4.4 Analysis

Chemical analyses of sediments were performed in the Vancouver laboratories of Bondar Clegg Ltd. using four independent methods.

4.4.1 Gold

Samples of 30 g were analysed for Au by fire-assay with subsequent determination of the fused product by atomic absorption spectrophotometry (AAS).

4.4.2 Major and trace cations

A suite of 34 major and trace cations (Ag, Cu, Pb, Zn, Mo, Ni, Co, Cd, Bi, As, Sb, Fe, Mn, Te, Ba, Cr, V, Sn, W, La, Al, Mg, Ca, Na, K, Sr, Y, Ga, Li, Nb, Sc, Ta, Ti, Zr) was simultaneously determined by inductively-coupled plasma emission spectroscopy (ICP-AES) following the digestion of 1.0 g aliquots in 100 ml of aqua-regia (ARISTAR). The use of aqua-regia rather than an HF-based total dissolution method reflects the superior peak/background responses to mineralisation obtained during orientation studies undertaken by the Misión Geológica Británica at Junín (Dunkley et al., 1997).

4.4.3 Metalloids

On account of the low resolution (5 mg/kg in solid) of metalloid analyses by ICP-AES, additional data for As and Sb were obtained by hydride-generation AAS. A flow-injection (FIA) introduction system by Nakashima (1979) facilitated the reduction of As to arsene and injection into the aspiration chamber simultaneously by merging a flow of 0.2% $NaBH_2$ with the sample carrier.

4.4.4 Mercury

Total Mercury was determined by cold-vapour AAS (CV-AAS) following aqua-regia digestion of 1.0 g sediment aliquots under hot-reflux.

5. QUALITY CONTROL

5.1 Sampling variance

For 31 elements the statistical variance attributable to at-site sediment heterogeneity and/or sampling bias was calculated for the entire Western Cordillera survey area using a modified analysis of variance (ANOVA) technique (Plant et al., 1975). Duplicate sediment samples acquired through repeat sampling of selected drainage sites (at a maximum frequency of 2 per 100) were analysed, and the results were used to determine sampling variance using the sums of squares technique (Bolviken and Sinding-Larsen, 1973). In instances where both duplicates from a single site yielded sub-detection limit values, the record was excluded from the calculation. Summary statistics are provided in Table 1. Statistical F-tests are not quoted, as the data do not fully satisfy the assumptions of conventional ANOVA analysis. It requires emphasis that the sampling variance data are themselves derived from the *analytical* determination of field duplicates. The values therefore assume interpretative significance only when in excess of the corresponding analytical precision threshold.

5.2 Analytical precision

Precision (p) is an index of the reproducibility of analytical determinations conventionally defined as:

$$p = \left(\frac{2s}{x}\right) * 100\%$$

The term is distinguishable from accuracy, which reflects the relationship between an individual determination or group of determinations and the true matrix composition. In exploration, indices of analytical precision are critical as they provide an insight into inter-comparability of data for individual samples or sample batches.

Analytical precision data for the 0°-1°S and 1-2°S Western Cordillera quadrangles were derived from two statistical exercises based on the duplicate analysis of aliquots of homogenized sediment (Plant et al., 1975; Thompson and Howarth, 1978). The first entailed a calculation of the variation of the standard deviation (s_c) across an empirically-defined concentration range (c) in accordance with the linear function:

$$s_c = s_0 + kc$$

where s_0 is the standard deviation at zero concentration and k is the gradient of the straight line. Values for s_0 and k were obtained by:

(i) Determination of mean $\frac{x^1+y^1}{2}$ and absolute difference (x^1-y^1) values for all duplicate pairs.

(ii) Ranking of duplicate pairs by ascending mean.

(iii) Calculation of the 'mean of means' and 'median of differences' for discrete groups of 11 duplicate pairs (8 groups = 88, with 3 discarded).

(iv) Regression of median against mean values determined in (iii) to yield s_0 (intercept) and k (gradient).

The second method utilised a series of precision control charts on which 90th and 99th percentile concordance lines were plotted for one or more pre-determined precision levels. Results derived from both methods, and utilised systematically in the quality-control of data for the 1°-2°S quadrangle, are summarised in Table 2.

Table 1. Sampling variance data, based on ANOVA analysis of duplicate samples from selected field stations within the Western Cordillera survey area.

Element	%variance	Element	%variance	Element	%variance	Element	%variance
Ag	7.1	**Sn**	15.2	**As**	3.1	**Ga**	11.6
Cu	3.1	**W**	21.7	**Sb**	6.9	**Y**	21.2
Pb	7.1	**La**	4.3	**Fe**	6.6	**Nb**	15.4
Zn	4.7	**Al**	3.6	**Mn**	7.1	**Sc**	16.0
Mo	25.0	**Mg**	7.1	**Bi**	17.5	**Ti**	4.4
Ni	12.4	**Ca**	12.5	**Ba**	3.2	**Zr**	12.1
Co	3.5	**Na**	12.2	**Cr**	9.3	**Hg**	21.7
Cd	4.2	**K**	9.4	**V**	4.9		

Table 2. Precision thresholds for selected elements applied for quality-control of analytical data for the 1°-2°S Western Cordillera quadrangle

Element	Est. precision %		Element	Est. precision %	
	M-1	M-2		M-1	M-2
Ag	-	25	**As**	9.76	7
Cu	5.86	15	**Sb**	21.34	15
Pb	5.64	20	**Mn**	6.24	7
Zn	7.16	10	**Fe**	-	15
Mo	12.61	10	**V**	28.32	25
Ni	11.44	20	**Cd**	25.61	10
Co	24.6	20	**Hg**	35.06	15
Ba	10.98	20	**Li**	23.95	5

5.3 Control standards

5.3.1 GIMP control standards

Three control standards derived from fluvial sediments within the project area (Junín River, J-1; Angamarca River, COR-1; hybrid sample, M-1) were characterised at the UK laboratories of the British Geological Survey by a combination of ICP-AES, ICP mass spectrometry (ICP-MS) and X-ray fluorescence (XRF) methods at the outset of the Western Cordillera survey (Table 3). With the exception of J-1 which contains anomalous concentrations of Cu (>96th %ile of the 1°-2°S dataset), plus moderately high As and Sb, these standards hold background concentrations of most elements of economic interest.

During the analysis of samples from the 1°-2°S area, additional control standards derived from mineralised localities at Ponce Enríquez (PE), Cerro Negro (CN), and a mixture of these plus lower background samples (M-2) were introduced. Repeat analyses undertaken by Bondar Clegg show the Ponce Enríquez standard to be highly anomalous with respect to a range of metals/metalloids, including As (mean 1476 mg/kg), Cu (mean 1062 mg/kg) and Au (mean 2.62 mg/kg). The Cerro Negro standard is strongly enriched in Cu (mean 398 mg/kg), Pb (125 mg/kg), Mo (44 mg/kg) and Sb (289 mg/kg) relative to the empirical dataset for the 1°-2°S area.

Table 3. BGS certification of control standards J-1, COR-1 and M-1, based on the mean of analysis by multiple techniques

Element	BGS value (ppm)			Element	BGS value (ppm)		
	J-1	COR-1	M-1		J-1	COR-1	M-1
Ag	<0.2	<0.2	<0.2	**As**	12.5	5.0	7.0
Cu	175	23	79.5	**Sb**	3.3	0.6	1.4
Pb	3.5	5.0	7.0	**Mn**	468	375	413
Zn	61	43	50.5	**Fe (%)**	4.9	8.1	7.0
Mo	1.6	0.5	1.0	**V**	150	293	226
Ni	10.5	18.5	14.0	**Sr**	28.5	61.0	48.0
Co	10.7	14.8	12.9	**Cd**	ND	1.0	0.5
Ba	74	64.5	73	**Li**	5.9	6.0	5.5
Cr	44.5	82.0	65.0				

Two sub-samples of three or more control standards were submitted blind to Bondar Clegg with each batch of 120 field samples. The resultant data provided a basis for evaluating (i) instrumental accuracy and (ii) temporal drift. The latter was evaluated independently of precision (4.2 above) as it commonly involves a systematic adjustment, thus amenable to correction. Analytical data for all Western Cordillera control standards are reported by Williams et al. (1997).

The impact of systematic instrumental drift on the Western Cordillera 1°-2°S dataset was evaluated using conventional time-series plots, as exemplified in Figs. 3-4. In rare instances in which control-standard values concurrently deviated by more than 2 standard deviations from the mean, an appropriate correction was applied. Examples exist in the time-series data shown for Zn, in which the values for standards submitted with analytical batches 22-24 are systematically depressed.

5.3.2 BGS Control standards

In addition to the project control standards described, BGS reference standards S13, S15, S24 and S3B were submitted for analysis by Bondar Clegg. These standards were derived from 100 BSI stream sediments from geologically varied British terrains. All have been analysed in several European laboratories by a combination of XRF, AAS, ICP-AES, ICP-MS and DRES methods. Inter-laboratory comparisons for these samples are provided by Williams et al. (1997). Relatively high values for elements such as Pb reflect the use by BGS of a total analytical technique (XRF) rather than the partial (aqua-regia digestion) method of Bondar Clegg.

5.4 Practical detection limits

With the exception of Au, analytical detection limits (LODs) provided by Bondar Clegg were not adopted for use in the validation of geochemical data as they do not account for the matrix influences typically encountered during the analysis of geological materials. Practical LODs for each element were instead determined using two methods. The first involved the replicated analysis of reference samples over a range of concentrations, and the regression of the standard deviation against the mean concentration for each value to yield a value of the standard deviation at zero concentration (s_0). A LOD of $3s_0$ was then calculated in accordance with UIPAC (1978). The second method involved the derivation of s_0 using the method of Thompson and Howarth (1978), as outlined in section 4.2. Results of LOD determinations derived specifically from the duplicate analysis of reference samples undertaken in conjunction with analyses of field samples from the 1°-2°S area are given in Table 4. Data for both methods are quoted, with the adopted value highlighted in each case.

Table 4. Bondar Clegg and independently determined analytical detection limits (adopted values highlighted). All values are in mg/kg unless otherwise indicated

Element	Bondar Clegg	Extrapolation Method	Thompson and Howarth
Ag	0.2	**1.0**	0.9
Au	0.05	-	-
As	1	1.86	**2.5**
Ba	1	**0.45**	8.0
Bi	5	**4**	4.0
Cd	0.2	0.066	**0.69**
Cr	1	**0.3**	3.0
Co	1	2.15	**3**
Cu	1	**2.65**	4
Fe	0.01%	**0.7%**	0.3%
Hg	0.01	0.03	**0.04**
Li	1	**0.8**	0.8
Mn	1	47	**35**
Mo	1	**0.77**	0.7
Ni	1	**1.38**	1
Pb	2	**5.1**	6.0
Sb	0.2	**1.9**	0.74
Zn	1	**5.0**	15.0

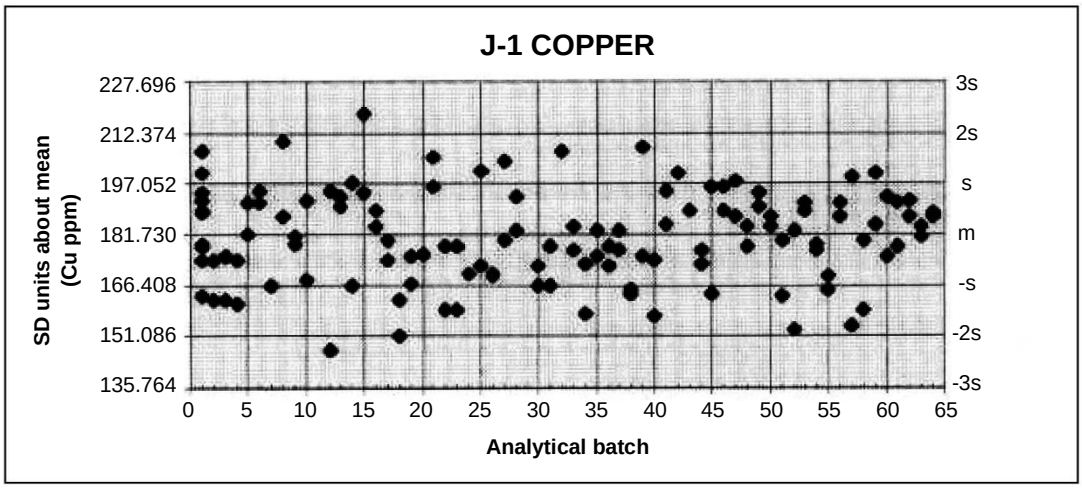

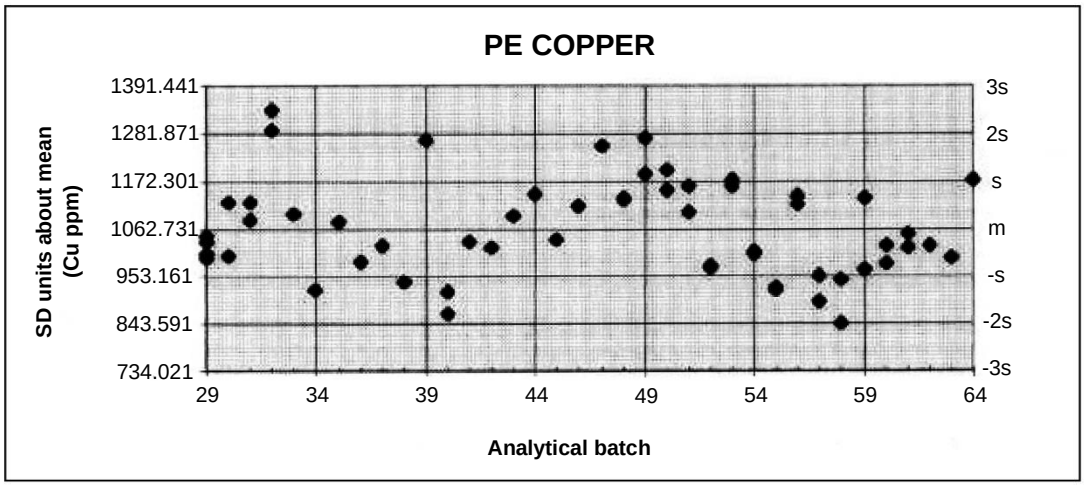

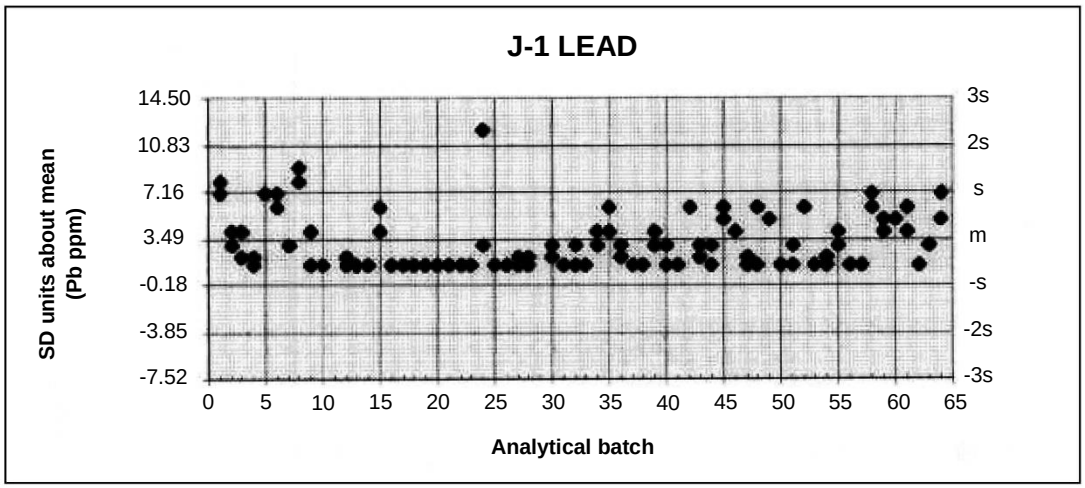

Figure 3. Copper and lead time-series control plots showing the results of replicate analyses of simultaneous duplicate pairs of Ecuadorian reference sediments. Correction of the empirical dataset is applied under the GIMP only in instances where BOTH samples within a duplicate pair deviate from the mean by >2SD for any individual sample batch.

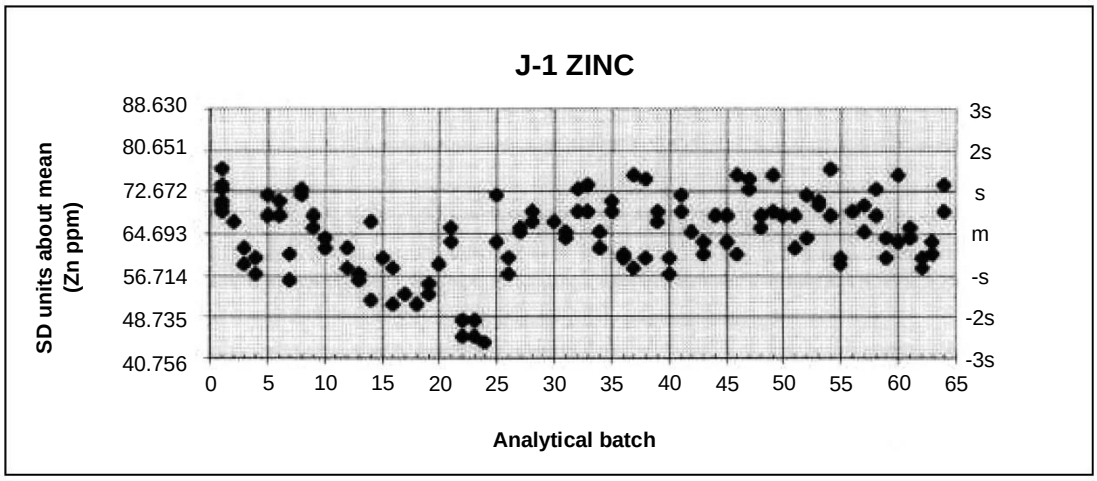

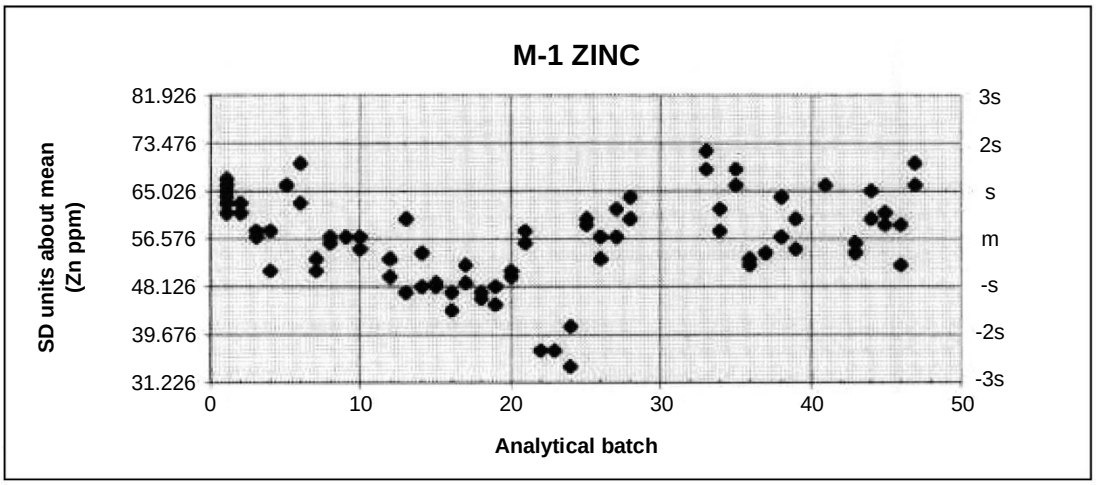

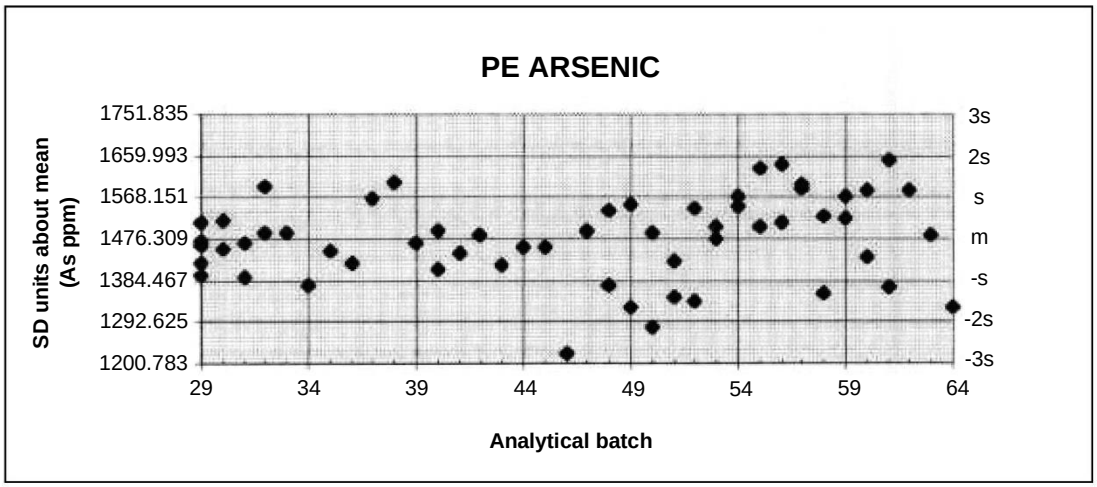

Figure 4. Zinc and arsenic time-series control plots showing the results of replicate analyses of simultaneous duplicate pairs of Ecuadorian reference sediments. Correction of the empirical dataset is applied under the GIMP only in instances where BOTH samples within a duplicate pair deviate from the mean by >2SD for any individual sample batch. An example is provided by the Zn data for batches 22-24.

6. RESULTS

6.1 Summary statistics

Descriptive geochemical statistics for the Western Cordillera 1°-2°S quadrangle are provided in Table 5. Cumulative frequency analysis of the data indicated that populations for most elements are skewed and poorly amenable to non-parametric analysis. Pearson (R) correlation analyses of log-normalised data (Table 6) highlight strong, lithologically controlled covariation of elements with strong mafic affinities. For Ni, Cr, Mg, Co, Fe, V, correlation coefficients typically exceed 0.4, with a maximum of 0.86 recorded for Fe vs. V. Zinc and Aluminum also show statistically significant though generally weaker covariation with this group. Common enrichment of Cu and Bi with Mo (in porphyry-style mineralisation) is indicated by R coefficients of ca. 0.35 for these pairs. Gold and its commonly utilised pathfinders As, Sb and Hg display no significant covariance.

6.2 Image production

Geochemical imagery for the Western Cordillera sector 1°-2°S (Figs. 5-7) was generated using an inverse-distance weighting (IDW) algorithm in the commercial exploration software package Interdex. The geological lines superimposed onto each image correspond to those used in Figure 2, which therefore provides an appropriate legend.

6.3 Lithogeochemical terranes

Figures 5-7 highlight a pronounced lithogeochemical contrast between the Macuchi Terrane (the Macuchi Unit and intrusive rocks emplaced therein) which dominates the western sector of the 1°-2°S quadrangle (west of ca. 725000 E) and the Angamarca, Zumbagua and more recent volcanic rocks (hereafter referred to as the Zumbagua Terrane) to the east. Mean and median values of Cu (64 and 52 mg/kg), V (219 and 193 mg/kg) and Al (2.99 and 2.95%) over the former are, for example, approximately twice those of the latter, while concentrations of Ca and Sr are a factor of two lower (see Tables 7-8). The Macuchi Terrane also yields a markedly higher mean Au value (25.25 vs. 11.89 μg/kg). While beyond the scope of this report, these terranes may thus warrant independent statistical interrogation as a basis for any detailed resource assessment.

Table 5. Descriptive statistics for geochemical data from the Western Cordillera sector 1°-2°S

	Count	Mean	Std. Dev	Min	Max	Median
Au	2150	21.10	110.54	3.33	3455.00	3.33
Ag	2150	0.53	0.24	0.66	2.70	0.66
Cu	2150	49.07	44.63	3.00	613.00	38.00
Pb	2150	6.92	9.50	1.33	288.50	5.00
Zn	2150	69.82	41.78	3.33	922.00	65.00
Mo	2150	1.39	1.35	0.66	26.00	0.90
Ni	2150	23.05	16.35	2.20	323.00	19.00
Co	2150	16.06	6.29	1.73	53.00	15.00
Cd	2150	0.41	0.34	0.13	10.40	0.46
Bi	2150	4.04	1.35	3.33	43.00	4.00
Fe	2150	4.93	2.33	0.05	10.00*	4.67
Mn	2150	611.15	393.86	22.66	10977.00	547.00
Te	2150	6.92	2.88	0.66	89.00	6.66
Ba	2150	118.52	68.33	3.60	1694.50	108.00
Cr	2150	53.19	37.21	2.46	669.00	44.00
V	2150	174.09	113.01	2.00	1029.00	150.00
Sn	2150	13.48	1.35	13.33	41.00	13.33
W	2150	13.37	0.64	13.33	28.00	13.33
La	2150	5.47	5.47	0.66	88.00	4.00
Al	2150	2.51	1.14	0.03	7.91	2.43
Mg	2150	0.60	0.38	0.01	3.82	0.52
Ca	2150	0.59	0.76	0.03	10.00*	0.45
Na	2150	0.05	0.03	0.01	0.29	0.04
K	2150	0.07	0.05	0.01	0.51	0.06
Sr	2150	45.73	30.09	-1.00	473.00	41.00
Y	2150	4.88	2.78	0.66	40.00	4.00
Ga	2150	4.00	3.45	1.33	47.00	3.00
Li	2150	6.79	4.76	0.80	53.00	6.00
Nb	2150	4.62	5.48	0.66	41.00	3.00
Sc	2150	6.18	4.10	3.33	30.00	3.33
Ta	2150	6.82	4.42	0.66	159.00	6.66
Ti	2150	0.16	0.06	0.01	0.79	0.15
Zr	2150	5.79	4.38	0.66	47.00	5.00
As	2150	7.17	31.46	0.66	1032.70	2.66
Sb	2150	1.06	0.50	0.13	7.90	1.26
Hg	2150	0.05	0.31	0.01	11.01	0.03

*signifies maximum reporting limit

Table 6. Western Cordillera sector 1°-2°S: Pearson correlation matrix

	Au	Ag	Cu	Pb	Zn	Mo	Ni	Co	Cd	Bi	Fe	Mn	Ba	Cr	V	Mg	Al	Ca	K	Sr	Ti	Zr	As	Sb	Hg
Au	***1.0000***	0.0015	0.0706	0.0609	0.1469	0.0417	0.0687	0.0962	-0.0006	-0.0121	0.0994	0.0317	0.0296	0.0636	0.0979	0.0611	0.0229	0.0004	0.0131	-0.0358	0.0576	-0.0093	0.0836	0.0358	0.0295
Ag	0.0015	***1.0000***	0.0481	0.2559	0.0705	0.1226	-0.0019	0.0049	**0.4347**	0.0856	0.0591	0.0011	-0.0331	0.0243	0.0453	0.0259	-0.0295	-0.0103	-0.0080	-0.0410	-0.0354	-0.0012	0.0067	0.0925	-0.0016
Cu	0.0706	0.0481	***1.0000***	0.1407	0.3103	0.3529	0.0605	0.3705	0.0669	0.1766	**0.4012**	0.2323	0.0946	0.0500	0.2594	0.3762	0.3512	-0.0020	**0.4056**	-0.1562	-0.0047	-0.0353	0.0182	0.1650	0.0006
Pb	0.0609	0.2559	0.1407	***1.0000***	0.3978	0.1642	0.01	0.086	0.0927	0.1658	0.1025	0.1583	0.1126	0.0161	0.0334	0.0695	0.1401	-0.0304	0.0257	-0.0964	-0.0221	0.0004	0.0547	0.1613	0.0450
Zn	0.1469	0.0705	0.3103	0.3978	***1.0000***	0.0889	0.1411	0.3752	0.1774	0.0632	0.3047	0.3462	0.2322	0.0724	0.1605	0.2628	0.3586	-0.0210	0.0526	-0.1224	0.1316	0.0642	0.1580	0.1200	0.0210
Mo	0.0417	0.1226	0.3529	0.1642	0.0889	***1.0000***	0.0235	0.0935	0.0273	0.3554	0.1971	0.1119	0.0127	0.0090	0.1191	0.0875	0.0744	-0.0061	0.1066	-0.2579	-0.0260	-0.0313	0.0265	0.2558	0.0283
Ni	0.0687	-0.0019	0.0605	0.0100	0.1411	0.0235	***1.0000***	**0.4926**	-0.0203	-0.0244	0.0692	0.0652	0.0747	**0.6719**	0.0016	**0.6161**	0.0933	0.1149	-0.1197	0.0331	0.2607	0.1812	-0.0081	0.0190	0.0044
Co	0.0962	0.0049	0.3705	0.0860	0.3752	0.0935	**0.4926**	***1.0000***	-0.0334	0.0393	**0.5928**	**0.4363**	0.2678	**0.4780**	**0.4758**	**0.5076**	**0.5718**	-0.0767	0.0889	-0.1527	**0.4284**	**0.4294**	-0.0167	0.0561	-0.0105
Cd	-0.0006	**0.4347**	0.0669	0.0927	0.1774	0.0273	-0.0203	-0.0334	***1.0000***	0.0937	-0.0333	0.0090	-0.0506	-0.0365	-0.0463	0.0059	-0.0514	-0.0081	-0.0118	-0.0232	-0.0630	-0.0543	0.2029	0.0521	0.0073
Bi	-0.0121	0.0856	0.1766	0.1658	0.0632	0.3554	-0.0244	0.0393	0.0937	***1.0000***	0.2294	0.1111	-0.0242	0.0245	0.1871	0.0495	0.0351	-0.0265	0.1116	-0.1599	-0.0195	-0.0777	0.0068	0.0723	-0.0040
Fe	0.0994	0.0591	**0.4012**	0.1025	0.3047	0.1971	0.0692	**0.5928**	-0.0333	0.2294	***1.0000***	0.3220	0.1054	0.3295	**0.8686**	0.2041	**0.4549**	-0.1951	0.2513	**-0.4081**	0.2535	0.1417	-0.0326	0.0406	-0.0135
Mn	0.0317	0.0011	0.2323	0.1583	0.3462	0.1119	0.0652	**0.4363**	0.0090	0.1111	0.3220	***1.0000***	0.3471	0.0390	0.1579	0.2301	**0.4689**	-0.0520	0.0637	-0.1239	0.1341	0.1591	0.0543	0.0189	-0.0076
Ba	0.0296	-0.0331	0.0946	0.1126	0.2322	0.0127	0.0747	0.2678	-0.0506	-0.0242	0.1054	0.3471	***1.0000***	-0.0240	0.0222	-0.0175	**0.4790**	-0.0012	0.0967	0.0369	0.2116	**0.4048**	-0.0245	-0.0408	0.0093
Cr	0.0636	0.0243	0.0500	0.0161	0.0724	0.0090	**0.6719**	**0.4780**	-0.0365	0.0245	0.3295	0.0390	-0.0240	***1.0000***	0.3092	**0.4953**	0.1180	-0.0148	-0.0528	-0.1274	0.2137	0.1302	-0.0433	-0.0343	-0.0113
V	0.0979	0.0453	0.2594	0.0334	0.1605	0.1191	0.0016	**0.4758**	-0.0463	0.1871	**0.8686**	0.1579	0.0222	0.3092	***1.0000***	0.0219	0.2388	-0.1958	0.1656	-0.3383	0.3198	0.1634	-0.0625	-0.1370	-0.0168
Mg	0.0611	0.0259	0.3762	0.0695	0.2628	0.0875	**0.6161**	**0.5076**	0.0059	0.0495	0.2041	0.2301	-0.0175	**0.4953**	0.0219	***1.0000***	0.3283	0.1097	0.1612	-0.0537	0.0437	-0.0260	-0.0231	0.0165	-0.0120
Al	0.0229	-0.0295	0.3512	0.1401	0.3586	0.0744	0.0933	**0.5718**	-0.0514	0.0351	**0.4549**	**0.4689**	**0.4790**	0.1180	0.2388	0.3283	***1.0000***	-0.1413	0.1661	-0.2010	0.2899	**0.4716**	-0.0283	-0.0331	-0.0252
Ca	0.0004	-0.0103	-0.0020	-0.0304	-0.0210	-0.0061	0.1149	-0.0767	-0.0081	-0.0265	-0.1951	-0.0520	-0.0012	-0.0148	-0.1958	0.1097	-0.1413	***1.0000***	-0.0428	**0.5227**	-0.1131	-0.0917	0.0159	0.0036	-0.0001
K	0.0131	-0.0080	**0.4056**	0.0257	0.0526	0.1066	-0.1197	0.0889	-0.0118	0.1116	0.2513	0.0637	0.0967	-0.0528	0.1656	0.1612	0.1661	-0.0428	***1.0000***	-0.0741	-0.0335	-0.0986	0.0010	0.0088	-0.0090
Sr	-0.0358	-0.0410	-0.1562	-0.0964	-0.1224	-0.2579	0.0331	-0.1527	-0.0232	-0.1599	**-0.4081**	-0.1239	0.0369	-0.1274	-0.3383	-0.0537	-0.2010	**0.5227**	-0.0741	***1.0000***	-0.0054	0.0690	0.0562	0.0113	-0.0089
Ti	0.0576	-0.0354	-0.0047	-0.0221	0.1316	-0.0260	0.2607	**0.4284**	-0.0630	-0.0195	0.2535	0.1341	0.2116	0.2137	0.3198	0.0437	0.2899	-0.1131	-0.0335	-0.0054	***1.0000***	**0.5291**	-0.0555	-0.0145	-0.0119
Zr	-0.0093	-0.0012	-0.0353	0.0004	0.0642	-0.0313	0.1812	**0.4294**	-0.0543	-0.0777	0.1417	0.1591	**0.4048**	0.1302	0.1634	-0.0260	**0.4716**	-0.0917	-0.0986	0.0690	**0.5291**	***1.0000***	-0.0442	-0.0069	-0.0170
As	0.0836	0.0067	0.0182	0.0547	0.1580	0.0265	-0.0081	-0.0167	0.2029	0.0068	-0.0326	0.0543	-0.0245	-0.0433	-0.0625	-0.0231	-0.0283	0.0159	0.0010	0.0562	-0.0555	-0.0442	***1.0000***	0.2232	0.0144
Sb	0.0358	0.0925	0.1650	0.1613	0.1200	0.2558	0.0190	0.0561	0.0521	0.0723	0.0406	0.0189	-0.0408	-0.0343	-0.137	0.0165	-0.0331	0.0036	0.0088	0.0113	-0.0145	-0.0069	0.2232	***1.0000***	0.0968
Hg	0.0295	-0.0016	0.0006	0.0450	0.0210	0.0283	0.0044	-0.0105	0.0073	-0.0040	-0.0135	-0.0076	0.0093	-0.0113	-0.0168	-0.0120	-0.0252	-0.0001	-0.0090	-0.0089	-0.0119	-0.0170	0.0144	0.0968	***1.0000***

2150 observations were used in this computation

6.4 Distribution of selected elements of economic significance

6.4.1 Copper

Cumulative probability analysis of the Cu data for the 1°-2°S quadrangle indicated an inflection in the population at the 98th percentile (ca. 160 mg/kg). Values in excess of this threshold typically occur independently of enrichment in other base-metals. Coincident Au enrichment is observed in only a few instances. All anomalous Cu values are confined to the Macuchi Terrane, for which a high background of ca. 38 mg/kg Cu has been calculated (50th percentile).

Known copper prospects are highlighted in several localities, almost all of porphyry style, associated with granitoid intrusions or intrusive margins. In the Río Chuquirahuas system, [713526-9887668 and 413462-9887523] values of 290 and 317 mg/kg Cu reflect disseminated sulphides hosted by a minor stock. Near El Corazón a value of 156 mg/kg Cu occurs in Quebrada Palmira [712632-9872390]. Several high Cu values (to 613 mg/kg) overlie weak porphyry mineralisation near the northern outcrop limit of the Chazo Juan intrusion [eg. 705729-9845483]. At the southern margin of the same pluton [eg. 707438-9815599] the Telimbela and Ashuaca Cu-Mo prospects are highlighted by Cu to 137 mg/kg with modest coincident enrichment of Au (33 μg/kg), As (34 mg/kg) and Sb (3.9 mg/kg). Over the Echeandía pluton [eg. 689099-9824037] values to 159 mg/kg Cu with attendant Au enrichment to 84 μg/kg demark the La Industria prospect. Near Santa Lucía, a rare polymetallic anomaly at 706112-9809091 (218 mg/kg Cu, 48 μg/kg Au, 1.8 mg/kg Ag, 288 mg/kg Pb, 472 mg/kg Zn, 13 mg/kg Bi and 1.8 mg/kg Cd) is related to the El Torneado porphyry target, formerly evaluated by JICA (1989-1991). Here Cu sulphides are reported both in the marginal facies of the Balzapamba intrusion and the hornfelsed Macuchi rocks to the north.

New potential targets indicated by drainage Cu data for the 1°-2°S quadrangle show a strong relationship with north-trending regional structures. The most notable occur along the Río Chimbo Fault south-east of San Pablo de Atenas, for example in Quebrada Las Palmas at 721807-9785023 (386 mg/kg Cu with 196 μg/kg Au, 18.5 mg/kg Mo and 1 mg/kg Cd) and Quebrada Yucapamba (534 mg/kg Cu, 436 mg/kg Zn, 3.5 mg/kg Cd). Additional anomalies with follow-up potential occur over Macuchi rocks between an outcrop of the Arrayanes Unit and the Chazo Juan intrusion (283 mg/kg Cu at 705269-9822488). New targets associated with granitoid margins are evident at the southern tip of the El Corazón intrusion north-west of Simiátug [72489-9859766] (330 mg/kg Cu with 26 mg/kg Mo and 71 mg/kg As), near the northern limit of the quadrangle at 714319-9882262 (210 mg/kg Cu, 369 μg/kg Au), and at the eastern contact of the Balzapamba intrusion near San Pablo de Atenas (198 mg/kg Cu, 1308 μg/kg Au, 33 mg/kg Te).

Table 7. Descriptive statistics for the Macuchi Terrane. Western Cordillera, sector 1°-2°S

	Count	Mean	Std. Dev	Min	Max	Median
Au	1245	25.25	128.20	3.33	3455.00	3.33
Ag	1245	0.51	0.25	0.13	2.70	0.66
Cu	1245	64.43	50.92	6.00	613.00	52.00
Pb	1245	7.83	8.64	1.33	150.00	6.00
Zn	1245	79.12	36.51	3.33	436.00	74.00
Mo	1245	1.58	1.63	0.66	26.00	0.90
Ni	1245	21.43	13.79	2.20	187.00	18.00
Co	1245	17.70	6.06	1.73	53.00	17.00
Cd	1245	0.41	0.41	0.13	10.40	0.46
Bi	1245	4.14	1.71	3.33	43.00	4.00
Fe	1245	6.19	1.98	0.05	10.00*	5.96
Mn	1245	688.77	291.85	22.66	2004.00	657.00
Te	1245	7.09	3.63	0.66	89.00	6.66
Ba	1245	120.73	54.70	3.60	415.00	112.00
Cr	1245	55.47	34.20	5.00	300.00	46.00
V	1245	219.74	118.05	2.00	1029.00	193.00
Sn	1245	13.58	1.74	13.33	41.00	13.33
W	1245	13.40	0.80	13.33	28.00	13.33
La	1245	6.29	6.55	0.66	88.00	4.00
Al	1245	2.99	1.03	0.03	7.91	2.95
Mg	1245	0.67	0.36	0.01	3.14	0.60
Ca	1245	0.44	0.25	0.03	2.55	0.38
Na	1245	0.04	0.02	0.01	0.17	0.03
K	1245	0.08	0.05	0.01	0.51	0.06
Sr	1245	33.68	16.47	-1.00	102.00	34.00
Y	1245	5.77	2.84	0.66	40.00	5.00
Ga	1245	4.54	3.71	1.33	39.00	4.00
Li	1245	6.93	3.66	0.80	46.00	6.00
Nb	1245	5.34	6.38	0.66	41.00	3.00
Sc	1245	7.57	4.57	3.33	30.00	6.00
Ta	1245	6.88	5.56	0.66	159.00	6.66
Ti	1245	0.16	0.06	0.01	0.79	0.15
Zr	1245	5.57	4.15	0.66	35.00	5.00
As	1245	7.01	32.11	0.66	1032.70	2.66
Sb	1245	1.03	0.55	0.13	7.90	1.26
Hg	1245	0.05	0.32	0.01	11.01	0.03

*signifies maximum reporting limit

Table 8. Descriptive statistics for the Zumbagua Terrane. Western Cordillera, sector 1°-2°S

	Count	Mean	Std. Dev	Min	Max	Median
Au	822	11.89	58.46	3.33	1180.00	3.33
Ag	822	0.59	0.18	0.13	1.80	0.66
Cu	822	27.91	20.38	3.00	218.00	22.00
Pb	822	5.56	10.88	1.33	288.50	4.00
Zn	822	53.73	45.01	3.33	922.00	45.00
Mo	822	1.16	0.77	0.66	6.00	0.90
Ni	822	25.93	19.78	2.20	323.00	21.00
Co	822	13.47	5.78	1.73	44.00	12.00
Cd	822	0.43	0.19	0.13	2.70	0.46
Bi	822	3.94	0.48	3.33	14.00	4.00
Fe	822	2.98	1.28	0.10	10.00*	2.73
Mn	822	493.69	495.72	22.66	10977.00	406.50
Te	822	6.69	1.32	0.66	37.00	6.66
Ba	822	108.64	81.83	14.00	1694.50	95.00
Cr	822	49.99	41.79	2.46	669.00	41.00
V	822	102.06	51.38	4.00	390.00	88.00
Sn	822	13.35	0.38	13.33	21.00	13.33
W	822	13.33	0.00	13.33	13.33	13.33
La	822	4.12	3.04	0.66	28.00	4.00
Al	822	1.67	0.73	0.07	7.00	1.53
Mg	822	0.53	0.39	0.01	3.82	0.44
Ca	822	0.84	1.15	0.09	10.00*	0.57
Na	822	0.08	0.03	0.01	0.29	0.08
K	822	0.05	0.03	0.01	0.25	0.05
Sr	822	64.63	36.92	-1.00	473.00	64.00
Y	822	3.37	1.85	0.66	11.00	3.00
Ga	822	3.01	2.67	1.33	47.00	2.00
Li	822	6.67	6.21	0.80	53.00	4.00
Nb	822	3.53	3.52	0.66	22.00	3.00
Sc	822	3.99	1.68	3.33	16.00	3.33
Ta	822	6.75	2.07	0.66	51.00	6.66
Ti	822	0.15	0.06	0.01	0.52	0.14
Zr	822	5.60	4.36	0.66	47.00	5.00
As	822	7.85	32.02	0.66	770.65	2.66
Sb	822	1.14	0.39	0.13	3.00	1.26
Hg	822	0.06	0.32	0.01	7.15	0.03

*signifies maximum reporting limit

6.4.2 Gold

A total of 33 anomalous Au values were resolved by cumulative probability analysis of the Au dataset, corresponding to uppermost ca. 1.5% of the population. Over 50% are associated with intrusive settings in the Macuchi Terrane, notably with minor stocks emplaced into basalts and basaltic andesites in the northwest of the mapped area. The highest recorded value (3455 μg/kg) is located at 707296-9889197 in Río Chuquiraguas, 5 km downstream of its bisection of a pyrite/chalcopyrite-bearing granodiorite intrusion 12 km north of El Corazón. A value of 392 μg/kg Au is recorded in the same drainage 3 km downstream of the intrusive contact at 710278-9888529. Neither site displays significant enrichment in base metals or metalloids. Quebrada Andoa, a north-flowing tributary of the Río Chuquiraguas, produced a value of 393 μg/kg Au with modest Cu enrichment (112 mg/kg) 1 km to the east of the same intrusion 7 km to the south, a value of 369 μg/kg, with attendant Cu enrichment to 210 mg/kg may be associated with weak porphyry mineralisation over an intrusive stock within basalts of the Macuchi Unit at 714319-9882202. In the south of the quadrangle, possible new targets close to the south-east margin of the Balzapamba intrusion are evident ca. 10 km north of Chillanes (1308 μg/kg Au with 33 mg/kg Te and 198 mg/kg Cu in Quebrada Juan León Mera at 714254-9793270; 845 μg/kg Au at 711486-9792787).

Hitherto undocumented Au mineralisation within the Río Chimbo Fault zone is signified by numerous sub-anomalous and anomalous Au values along the trace of the fault for a distance of ca. 20 km east of San Pablo de Atenas. The highest values are recorded in Quebrada Pindorata (1638 μg/kg Au with 273 mg/kg As and 0.134 mg/kg Hg) at 721880-9786328, Río del Alumbre (326 μg/kg Au) at 720523-9782541 and Río Chimbo (399 μg/kg Au with 303 mg/kg As) at 720466-9779112. These tributaries emanate from both east (i.e. from Pallatanga Unit and Yunguilla sources) and west (i.e. a Macuchi Unit source) of the north-south trending fault, thus strongly suggesting a structural rather than lithological control. Near Cani, a value of 639 μg/kg Au with 109 mg/kg Cu and 43 mg/kg As occurs on the parallel Cani Fault at 724094-9805424. The widely variable As enrichment in this area, plus the occurrence of at least two independent Cu-Mo anomalies (with minimal Au-metalloid enrichment), infers more than one phase or style of mineralisation, probably with contrasting temperature regimes.

Alluvial or colluvial Au occurs widely within the Quaternary cover which fringes the western margin of the Western Cordillera, much of which can be sourced with confidence to intrusion-related mineralisation within the Macuchi Terrane. In the northwestern sector of the mapped area examples include Estero de Oro (934 μg/kg Au at 691549-9879919) south of Estero de Damas, Estero del Guabo (1335 μg/kg Au with 1.48 mg/kg Hg at 686782-9875049; 471 μg/kg Au at 690265-9872266), Río Sillagua (339 μg/kg Au at 703108-9876253; 492 μg/kg Au at 701895-9873346), Q. Palmiro (764 μg/kg Au at 712343-9872660) and Río Naves Chico (282 μg/kg Au at 688855-9855353). Further south, 283 μg/kg Au is recorded at 681881-9831774 west of La Industria, and values to 303 μg/kg Au occur 10-15 km north of Montalvo in drainage systems emanating from the Telimbela prospect. The presence of Hg in Estero de Guabo sediments is attributed to contamination from artisanal mining.

Few Au anomalies occur over the Zumbagua and more recent volcanic rocks which dominate the eastern half of the 1°-2°S quadrangle. The most prospective occurs in an area of known travertine mineralisation 723064-9839358 south of Salinas (1180 μg/kg Au). A value of 514 μg/kg Au with no attendant base metal or metalloid enrichment also occurs at 735498-9797187 northeast of Angamarca. Over the Yunguilla Unit, a value of 645 μg/kg is recorded in Quebrada Mocata at 730439-9779053.

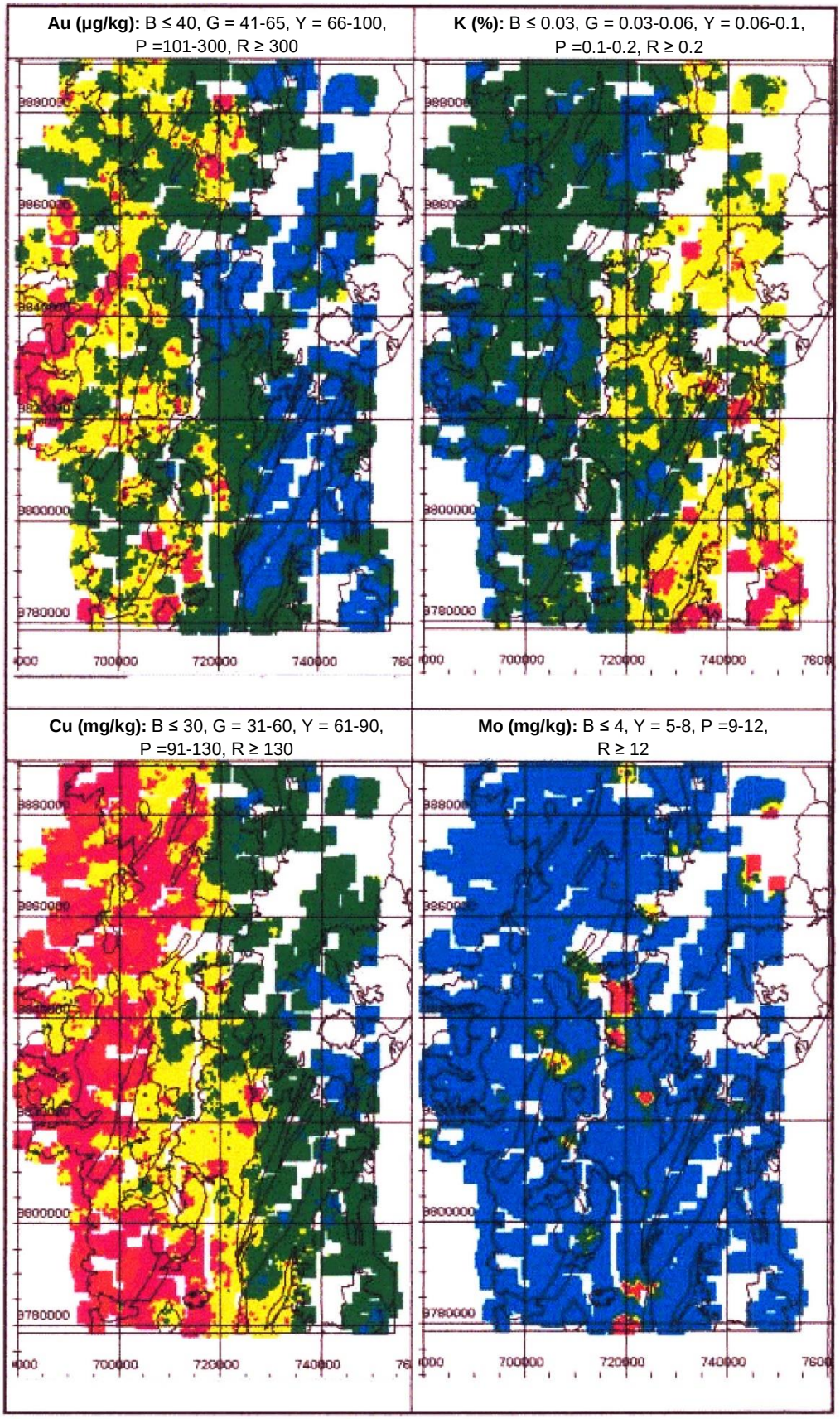

Figure 5. IDW grids for Au, K, Cu and Mo over the 1°-2°S sector of the Western Cordillera

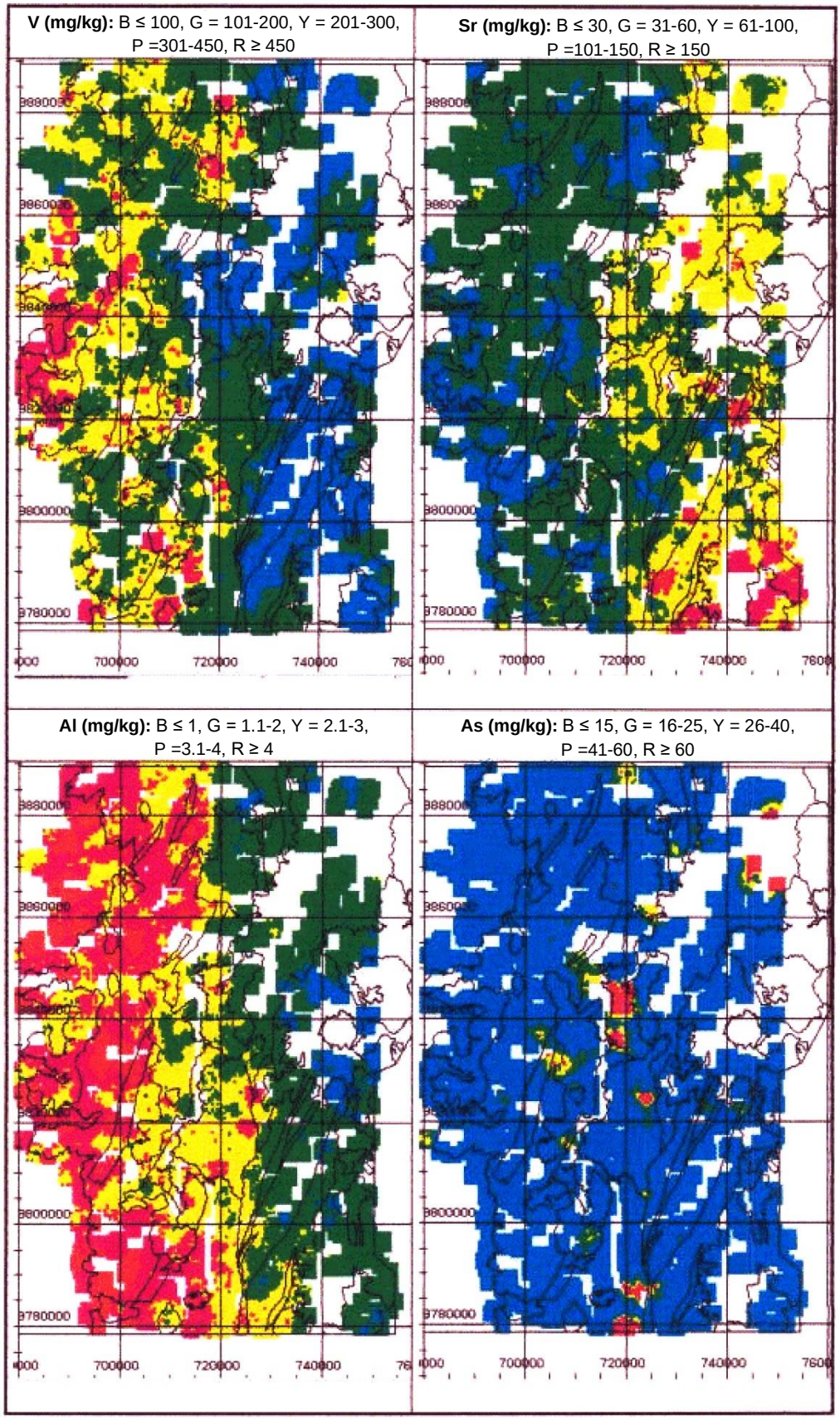

Figure 6. IDW grids for V, Sr, Al and As over the 1°-2°S sector of the Western Cordillera

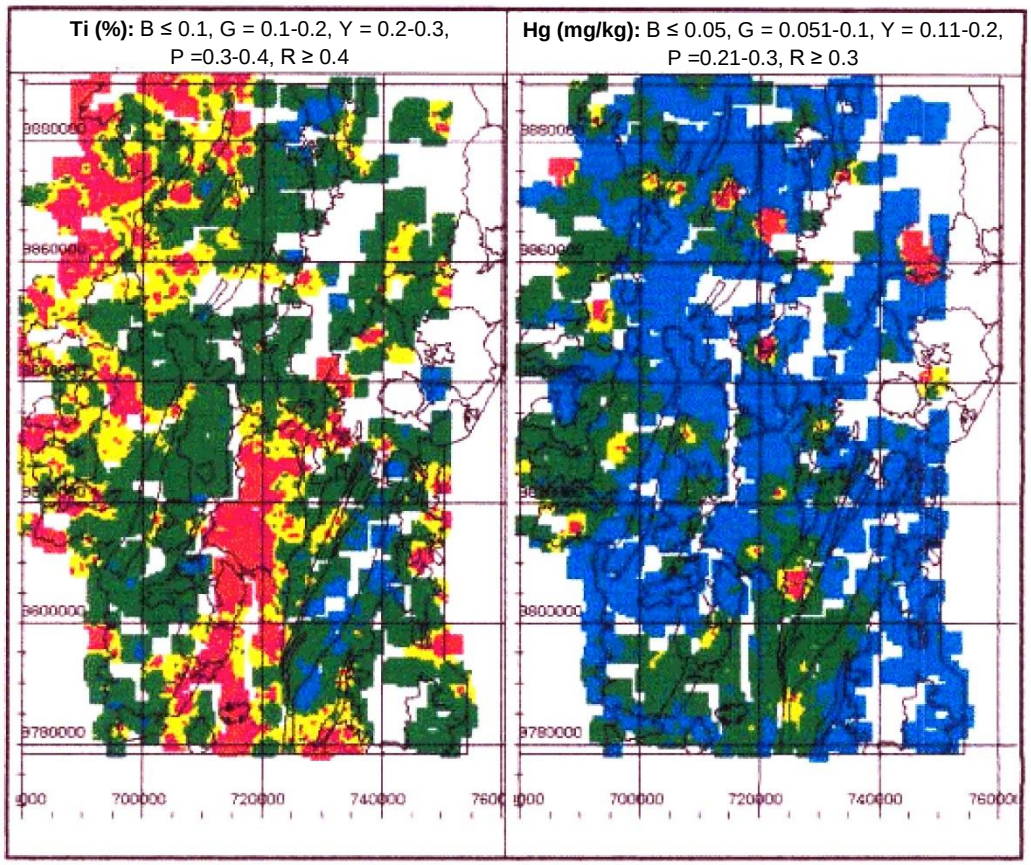

Figure 7. IDW grids for Ti and Hg over the 1°-2°S sector of the Western Cordillera

6.4.3 Mercury

Anomalous Hg values (>0.4 mg/kg) within the 1°-2°S sector of the Western Cordillera occur primarily within three discrete settings:

(i) Alluvial or colluvial deposits to the west of the Macuchi Terrane.
(ii) Associated with granitoids or intrusive margins.
(iii) Associated with post-Miocene hot springs.

The distribution of anomalous values differs from other elements of economic significance, being more evenly distributed between the Macuchi and Zumbagua terranes. Few of the high values described can be related to known mineralisation.

Anomalies associated with alluvial/colluvial settings are well exemplified in the northwest of the region, notably in Estero del Guabo (1.4 mg/kg Hg at 686782-9875049) and Río Sillagua (0.46 mg/kg Hg at 701895-9873346). These features are probably anthropogenic, arising from gold amalgamation processes undertaken by small-scale prospectors.

The El Corazón intrusion hosts an intense Hg anomaly of 11.00 mg/kg in the Río Simiátug [721936-9865486]. Over the southern sector of the Balzapamba pluton, a value of 0.46 mg/kg Hg is accompanied by modestly elevated As and Sb. Neither anomaly appears to be related to documented mineralisation.

Anomalous Hg values over the Zumbagua Group occur close to its contact with the overlying Chimborazo lavas. The highest such value (7.14 mg/kg) is recorded at 747286-9858735 in Q. Cubillín, a minor tributary of the Río Ambato. Additional values of 4.89 mg/kg, 0.51 mg/kg and 0.70 mg/kg occur immediately north of the Río Ambato at 746070-9862872, 745950-9861680 and 746044-9861713 respectively. To the southwest, a value of 1.27 mg/kg Hg occupies a similar lithological, though possibly fault-controlled setting over the Río Chimbo lineament [6912581-9850767]. These anomalies show no coincident metalloid and/or base metal enrichment and their locations are wholly consistent with precipitation from hydrothermal spring emanations at the base of the Chimborazo lava pile. A value of 1.41 mg/kg with 55 mg/kg As denotes a documented low sulphidation hydrothermal system at Salinas [720627-9844728].

Mercury anomalies which do not fall into one of the three above-noted settings include a value of 2.21 mg/kg with 1.55 mg/kg Cd and 16.3 mg/kg Te over the Angamarca Group at 725999-9806567, and a value of 0.50 mg/kg Hg over Quaternary volcanics of the Río El Batán catchment, [719854-9812097], the latter possibly associated with mineralisation along the Río Chimbo lineament.

6.4.4 Silver

Over 99% of geochemical samples from the 1°-2°S quadrangle yielded Ag values below the 1 mg/kg analytical detection limit. The distribution of higher values is associated with base metal rather than Au enrichment, and is almost exclusively related to intrusive margins within the Macuchi Terrane. Anomalies associated with known prospects occur in Río Telimbela (2.7 mg/kg Ag with 89 mg/kg Te and 6.1 mg/kg Cd at 691896-9816039) close to Cerro Samama, and near the El Torneado porphyry (1.8 mg/kg Ag with 218 mg/kg Cu, 48 μg/kg Au, 288 mg/kg Pb, 472 mg/kg Zn, 13 mg/kg Bi and 1.8 mg/kg Cd at 706112-9809091 in Quebrada Las Juntas). Possible new targets are signified by 1 mg/kg Ag with 330 mg/kg Cu, 26 mg/kg Mo and 71 mg/kg As in Quebrada Chigue at the southern tip of the El Corazón intrusion [724899-9859766], and in Quebrada Payayacu (1.6 mg/kg Ag with 63 mg/kg Te and 5 mg/kg Cd at 707984-9831410) and Río San Dolomi (1.2 mg/kg Ag at 706406-9826142) on the western side of the Chazo Juan intrusion. Alluvial Ag, almost certainly derived from the Santa Rita-Yatubi prospect, is recorded south-west of La Industria at 690107-9823452 (1.4 mg/kg Ag with 6 mg/kg Bi).

6.4.5 Arsenic

The mean abundance of As recorded over the 1°-2°S quadrangle is low relative to the more southerly sectors of the Western Cordillera (e.g. Williams et al., 1997; 1998). Statistically anomalous values (>99%ile) thus extend upward of only ca. 55 mg/kg. Their distribution shows only a weak, sporadic association with Au. Three principal anomalous settings are identifiable:

(i) Intrusions or contact alteration zones (generally carrying pyrite with or without chalcopyrite and other minor base-metal sulphides) within the Macuchi Terrane.
(ii) Low-sulphidation epithermal systems/sinters within the Zumbagua Terrane.
(iii) Mineralisation along the Chimbo lineament bisecting both the Macuchi and Zumbagua terranes.

Probable Cu-Mo mineralisation at the southern margin of the El Corazón intrusion carries 71 mg/kg As (with 6 mg/kg Sb, 330 mg/kg Cu and 26 mg/kg Mo) at 724899-9859766. To the north-west, the highest As value of the dataset (1032 mg/kg) occurs with no attendant Au or base-metal enrichment in a zone of alteration between two minor granitoid stocks [713935-9841187]. Most other intrusive-related As anomalies are associated with the Chazo Juan pluton, for example at 707990-9831293 (62 mg/kg As with 0.46 mg/kg Hg), and at the western contact at 706100-9830618 (69 mg/kg As with 7 mg/kg Sb).

Known travertine and epithermal Au-Ag mineralisation at Salinas is marked by As anomalies to 770 mg/kg at 720627-9844728 and 718918-9844635. Similar sinter-type emanations are indicated by a succession of analogous (universally Au and base-metal poor) anomalies extending some 7 km southward along the Río Salinas (e.g. 200 mg/kg As at 719054-9842058; 59 mg/kg As at 718075-9839385; 125 mg/kg As at 719268-9835689).

In the south of the mapped area, the Chimbo lineament yields strong As anomalies at 720466-9779112 (303 mg/kg As with 399 μg/kg Au) and 721880-9786328 east of Chillanes (273 mg/kg As with 1638 μg/kg Au). Following the trace of the fault northward over the Quaternary volcanics of the Guaranda area, a value of 250 mg/kg As is recorded in Q. Lillohuaicu (723894-9824390). Over the Zumbagua Group, values of 67 mg/kg As at 744456-9867253, 84 mg/kg As at 745365-9869992 and 120 mg/kg As at 748816-9880499 are constrained by the same structure.

6.5 Summary of economic potential

Table 9 summarises the principal exploration targets in the 1°-2°S sector of the Western Cordillera highlighted by the drainage reconnaissance dataset compiled under PRODEMINCA sub-component 3.4. Seven formerly undocumented localities are listed, all of which warrant further investigation. The San Pablo de Atenas, Quebrada Chigue and Quebrada Payayacu anomalies probably highlight mineralisation of the style previously recognised as dominant within the 1°-2°S quadrangle (i.e. porphyry-type or vein and dissemination mineralisation at the contact of major granitoids with the volcanoclastics of the Macuchi Unit). Of these, the Quebrada Chigue anomaly has, to date, proved particularly difficult to constrain as a result of access restrictions imposed by indigenous communities.

The identification of additional geochemical targets unassociated with intrusive rocks, but showing a strong regional structural control, may prompt significant re-evaluation of exploration strategies previously applied within the 1°-2°S quadrangle. The importance of the Chimbo lineament as a conduit for hydrothermal fluids is signified by the presence of As anomalies along a ca. 90 km strike length. It is, however, notable that attendant enrichment of Au and/or base metals occur exclusively within the Macuchi Terrane. This trend may indicate some lithological or 'crustal reservoir' control on the composition of mineralizing fluids, such as described by Plant et al. (1987) in their explanation of the distribution of Au mineralisation in the Dalradian of Scotland.

Table 9. Summary of possible geochemical targets in the Western Cordillera, sector 1°-2°S. Formerly undocumented localities are shown in bold. Note: coordinates correspond to areas of interest rather than specific drainage sampling sites.

Site	UTMX	UTMY	Signature	Mineralization
R. Chuquirahuas	713	9887	Cu	Porphyry
Chazo Juan	715	9845	Cu	Porphyry
Telimbela-Ashuaca	715	9815	Cu (Au, As)	Porphyry
La Industria	691	9827	Cu (Au)	Porphyry
El Torneado	706	9809	Cu (Au, Ag, Pb, Bi)	Vein and Stockwork
S. Pablo de Atenas	**714**	**9793**	**Au (Cu, Te)**	**Intrusive margin**
Chimbo 1	**721**	**9780**	**Au (As, Hg)**	**Epithermal**
Chimbo 2	**721**	**9785**	**Cu (Au, Mo)**	**Epi-mesothermal**
Cañi	**724**	**9805**	**Au (Cu, As)**	**Epithermal**
Salinas	720	9845	Au (As)	Low sulphidation epithermal
Río Ambato	**745**	**9863**	**Hg**	**Sinter**
Cerro Samama	689	9817	Ag (Te, Cd)	Mesothermal veins
Q. Chigue	**724**	**9859**	**Cu (Mo, Ag, As)**	**Porphyry?**
Q. Payayacu	**707**	**9831**	**Ag (Te, Cd)**	**Intrusive margin**

Strong mercury anomalies, with no coincident enrichment of precious or base-metals, such as those that occur on the northern flank of Río Ambato have been recorded in several other localities in the Western Cordillera, often constituting the outermost geochemical expression of diatreme or caldera-related hydrothermal systems. At Quimsacocha and Cerro Plancharumi, higher temperature Au and base-metal sulphide assemblages have been observed within a few kilometres of Hg anomalies of this type. While possibly associated with barren hot spring emanations from the Chimborazo centre, the Hg-rich geochemical signatures observed in drainage sediments of several Río Ambato tributaries may, therefore, warrant additional investigation.

6.6 Additional data applications

The wider applications of the regional geochemical data compiled for the Western Cordillera in fields such as environmental impact assessment, land use planning and the derivation of pragmatic environmental quality guidelines are fully recognised by PRODEMINCA, and have been outlined in detail by Williams et al. (1997; 1999). Within the context of the 1°-2°S quadrangle, the value of the dataset as a baseline against which the impacts of future mining and related industrial activities may be assessed is particularly considerable, given the strictly limited extent of historical or ongoing activity in this sector.

Within the structure of PRODEMINCA, probable areas of application for geochemical reconnaissance data compiled under sub-component 3.4 may include Policy Development (sub-component 2.3), Monitoring of Pollution and Health Related to Mining Activities (sub-component 3.1), Containment and Neutralization of Hazardous Mining Wastes (sub-component 3.2), Geological Mapping (sub-component 3.3), and Assessment of Ore Districts (sub-component 3.5). Data accessibility has been facilitated to the greatest possible extent under the current programme by the adoption of an Oracle database and Intergraph GIS, compatible with IT systems used under all other technical PRODEMINCA sub-components.

7. CONCLUDING STATEMENT

The central function of this document as a methodological/data overview is outlined in section 1. Following the release in April 1999 of digital geochemical data for the 1°-2°S sector of the Western Cordillera, the strategic and economic return will be determined largely by private sector interest. The demand for the involvement of CODIGEM, DINAPA, DINAMI and other government departments in data management, the provision of multi-thematic datasets and interpretive guidance will, however, remain. This longer-term public-sector contribution may ultimately be no less important than private investment in achieving the central PRODEMINCA goal of sustainable development of Ecuador's metalliferous minerals sector.

8. BIBLIOGRAPHY

ASPDEN J. A., LITHERLAND M., DUQUE P., SALAZAR E. BERMÚDEZ R. y VITERI F. (1987) Un nuevo cinturón ofiolítico en la Cordillera Real, Ecuador y su posible significado regional. Politécnica, XII, 2, 81-93.

AUCOTT J. W., PUIG C., QUEVEDO L., and BÁEZ N. (1979) Exploración geoquímica regional en el centro occidental del Ecuador (Proyecto San Miguel). Institute of Geological Sciences, Nottingham UK.

BALDOCK J. W. (1982) Geología del Ecuador. Boletín de la explicación del mapa geológico (1:1000000) de la República del Ecuador. Ministerio de Recursos Naturales y Energéticos, Quito, 54pp.

BOLVIKEN B. and SINDING-LARSEN B. (1973) Total error and other criteria in the interpretation of stream sediment data. In: Geochemical Exploration 1972 (London: Institution of Mining and Metallurgy).

BRITISH GEOLOGICAL SURVEY and CORPORACIÓN DE DESARROLLO e INVESTIGACIÓN GEOLÓGICO, MINERO y METALÚRGICO (1993) National geological map of Ecuador, scale 1:1000000, Nottingham (UK) and Quito (Litherland M., Zamora A. and Egüez A.).

DARNLEY A. G., BJORKLUND A., BOLVIKEN B., GUSTAVSSON N. and KOVAL P. (1995) A global geochemical database: Recommendations for international geochemical mapping. Final report of IGCP project 259. UNESCO, Paris.

DIRECCIÓN NACIONAL DE GEOLOGÍA Y MINAS (1978) Hoja Geológica de Ambato (68) 1:100000 scale.

DIRECCIÓN NACIONAL DE GEOLOGÍA Y MINAS and INSTITUTE OF GEOLOGICAL SCIENCES (1982) Mapa Geológico Nacional de la República del Ecuador, escala 1:1000000 (Baldock J. W. and Longo R.), Quito.

DUNKLEY P. N. and GAIBOR A. (1997) Geology of the area between 2 and 3 degrees south. Western Cordillera, Ecuador. Report No. 2. Proyecto de Desarrollo Minero y Control Ambiental, Programa de Información y Cartografía Geológica.

DUNKLEY P. N., GAIBOR A. and BOLAÑOS J. E. (1997) Geochemical orientation survey, Río Junín. Geological Information Mapping Programme (GIMP) Report No. 5. World Bank Mining Development and Environmental Control Project (PRODEMINCA), Misión Geológica Británica, CODIGEM, Quito, Ecuador.

EGÜEZ A. (1986) Evolution Cénozoïque de la Cordillère Occidentale Septentrional d’Equateur (0°15’S o 1°10’S). Les mineralisation associées. Unpublished PhD Thésis ; Université Pierre et Marie Curie, Paris 116p.

GARRETT R. G. (1983) Sampling methodology. In: Howarth R. J. Ed. Handbook of exploration geochemistry Volume 2: Statistics and data analysis in geochemical prospecting. Chapter 4, 83-111. Elsevier, London.

HALL M. L. and MOTHES P. A. (1994) Tefroestratigrafía holocénica de los volcanes principales del valle interandino, Ecuador. p. 47-68. In: El Contexto Geológico del Espacio Físico Ecuatoriano (ed. R. Marocco). Colegio de Geógrafos del Ecuador, Quito, Ecuador. 113p.

HENDERSON W. G. (1979) Cretaceous to Eocene volcanic arc activity in the Andes of northern Ecuador. Journal of the Geological Society of London, 136, 367-378.

HUGHES R. A. and BERMÚDEZ R. A. (1997) Geology of the area between 1 degree south and the equator, Western Cordillera, Ecuador. Report No. 4. Proyecto de Desarrollo Minero y Control Ambiental, Programa de Información Cartográfica y Geológica.

JAPAN INTERNATIONAL COOPERATION AGENCY (1989) Report on the mineral exploration in the Bolívar area, Republic of Ecuador, Phase I CODIGEM, Quito.

JAPAN INTERNATIONAL COOPERATION AGENCY (1990) Report on the mineral exploration in the Bolívar area, Republic of Ecuador, Phase II CODIGEM, Quito.

JAPAN INTERNATIONAL COOPERATION AGENCY (1991) Report on the mineral exploration in the Bolívar area, Republic of Ecuador, Phase III CODIGEM, Quito.

KENNERLEY J. B. (1973) Geology of the Loja Province, Southern Ecuador. Institute of Geological Sciences, Overseas Geology and Mineral Resources, 23, 34p.

MCCOURT W., ASPDEN J. A. and BROOK M. (1984) New geological and geochronological data from the Colombian Andes: Continental growth by multiple accretion. Journal of the Geological Society of London, 141, 831-845.

MCCOURT W., MUÑOZ C. A. and VILLEGAS H. (1991) Regional geology and gold potential of the Guapi-Napi drainage basin and the upper Timbiqui river, Department of Cauca SW Colombia. BGS Overseas Geology Series, Technical Report WC/90/34, 62p.

MCCOURT W., DUQUE P. and PILATASIG L. (1997) Geology of the Cordillera Occidental of Ecuador between 1° and 2° S. Geological Information Mapping Programme (GIMP) Report No. 3. World Bank Mining Development and Environmental Control Project (PRODEMINCA). Misión Geológica Británica, CODIGEM, Quito, Ecuador.

PEARCE J. A., HARRIS N. B. W. and TINDLE A. G. (1984) Trace element discrimination diagrams for the tectonic interpretation of granitic rocks. Journal of Petrology, 25, 956-983.

PLANT W. C. (1973) A random numbering system for geochemical samples. Transactions of the Institution of Mining and Metallurgy, Section b. 83.

PLANT J. A. and MOORE P. J. (1979) Regional geochemical mapping and interpretation in Britain. Philosophical Transactions of the Royal Society of London, Vol. 288, 95-112.

PLANT J. A., JEFFREY J. K., GRILL E. and FAGE C. (1975) The systematic determination of error, accuracy and precision in geochemical exploration data. Journal of Geochemical Exploration, Vol. 4, 467-486.

PLANT J. A., BREWARD N., FORREST M. D. and SMITH R. T. (1989) The gold pathfinder elements As, Sb and Bi – their distribution and significance in the south-west highlands of Scotland. Transactions of the Institution of Mining and Metallurgy (B), 98, 91-101.

THALMANN H. E. (1946) Micropalaeontology of Upper Cretaceous and Paleocene in Western Ecuador. Bulletin of the American Association of Petroleum Geologists, 30, 337-347.

THOMPSON M. and HOWARTH R. J. (1978) A new approach to the estimation of analytical precision. Journal of Geochemical Exploration, 9, 23-30.

WHALEN J. B., CURRIE K. L. and CHAPPELL B. W. (1987) A-type granites: geochemical characteristics, discrimination and petrogenesis. Contributions Mineralogy and Petrology, 95, 407-419.

WILLIAMS T. M., DUNKLEY P. N. and GAIBOR A. (1997) Geochemical reconnaissance Survey of the Cordillera Occidental of Ecuador between 2°-3°S. Geological Information Mappings Programme (GIMP) Report No. 7. World Bank Mining Development and Environmental Control Project (PRODEMINCA), Misión Geológica Británica, CODIGEM, Quito, Ecuador.

WILLIAMS T. M., CRUZ E., ACITIMBAY V., DUNKLEY P. N., GABOR A., LÓPEZ E., BÁEZ N. and ASPDEN J. A. (1999) Regional geochemical reconnaissance of the Cordillera Occidental of Ecuador: economic and environmental applications. Applied Geochemistry (in press).